C.P. No. 1122

C.P. No. 1122

MINISTRY OF TECHNOLOGY

AERONAUTICAL RESEARCH COUNCIL

CURRENT PAPERS

Tests at a Mach Number of 2·0 on a Rectangular, Twin-Duct Air Intake with Variable Geometry, Situated in the Flow Field of a Slender Wing

by

M. D. Dobson

Aerodynamics Dept, R.A.E., Bedford

LONDON: HER MAJESTY'S STATIONERY OFFICE

1970

PRICE *10s 0d* [*50p*] NET

U.D.C. 533.693.3 : 621.43.033.2 : 533.693.49 : 532.526

C.P. No. 1122
December 1968

TESTS AT A MACH NUMBER OF 2.0 ON A RECTANGULAR, TWIN-DUCT AIR INTAKE WITH VARIABLE GEOMETRY, SITUATED IN THE FLOW FIELD OF A SLENDER WING

by

M. D. Dobson

Aerodynamics Department, R.A.E., Bedford

SUMMARY

The tests were made in the 3ft x 3ft tunnel to assess the performance of a rectangular twin-duct intake, including effects of limited immersion of the intake into a wing boundary layer. The effects in one duct, arising from interference caused by varying the flow through the other, have also been investigated.

Partial immersion of the intake into the wing boundary layer causes little degradation of the intake performance and indeed, small increases of pressure recovery are noted.

It is inferred from the results that interference effects may be sensitive to small crossflow angles at the intake. Smaller margins of mass flow reduction without interference are observed when the windward duct is throttled. The design of the leading edge of the wall which separates the two ducts (splitter), affects the interference characteristics and the present design is shown to be a considerable improvement over shapes tested previously.

---

* Replaces R.A.E. Technical Report 68285 - A.R.C. 31118.

CONTENTS

1 INTRODUCTION

In Ref.1 results were presented of tests made on a rectangular, twin duct air intake in isolation in the uniform flow field of a wind tunnel. The intake was typical of the type proposed for a supersonic transport aircraft and as such, would be required to operate in the flow field generated by a wing. A suitable slender half-wing has therefore been made and the intake mounted beneath it.

Results presented here are for the intake in the flow field of the wing at near cruise incidence, at a free stream Mach number of 2.0 and a Reynolds number, based on inlet capture height, of 0.64×10^6.

2 EXPERIMENTAL DETAILS

2.1 Wing*

The intake mounted onto the wing is shown in Figs.1 and 2. The wing, which was to 1/12 scale, was not a complete half-wing and the part of the planform represented is indicated in Fig.2. Chord AA (Fig.2) was placed on the tunnel floor and thus the inboard part of the wing was immersed into the tunnel boundary layer. The tunnel floor boundary layer varies in thickness from about 1.5 in at the position of the model root leading edge, to about 1.6 in at the longitudinal position of the intake.

The attitude selected for the tests was an incidence of the body datum of 3.5°. Other wind tunnel tests on a complete model of this configuration, had shown that this value of incidence produced a cruise C_L of 0.1 at a Mach number of 2.2.

2.2 Intake

The intake and nacelle was that used in the tests of Ref.1. All the components described in that reference were available for the present tests but to comply with the current aircraft design, a modification to the intake, involving the removal of the internal compression (internal wedge) on the

---

*The wing design is one of the Concorde series and designated "sixth wing". This was in fact, the first configuration after a 7% increase in linear dimensions had been introduced. Changes have subsequently been made for the prototype aircraft design.

outer side walls had been made, Fig.3, (cf. Fig.1, Ref.1). Also a design change had been made to the leading edge of the wall dividing the ducts, to that shown in Fig.3. This is referred to as splitter IV. The compression geometry and throat bleed arrangement (configuration A0 of Ref.1) are shown in Fig.4.

The planform position of the nacelle on the wing is as defined in Ref.2, with its centre line toed in at 2° 46'. The whole nacelle could be moved in a direction normal to the wing surface so that varying amounts of wing boundary layer could be ingested into the intake. A cavity in the wing surface above the nacelle ensured that the wing boundary layer air could flow unhindered back into the tunnel stream. No attempt was made to reproduce the boundary layer diverter designed for the full scale aircraft.

Difficulties in setting the angle of the nacelle in a pitch sense relative to a datum on the wing, resulted in an uncertainty of $\pm\frac{1}{2}^{\circ}$.

3 CALIBRATION OF WING FLOW

Before the intake was mounted onto the wing measurements were made of the local flow direction and Mach number distribution at the position of the intake compression surface leading edge, over the capture area of the intake. Wing boundary layer thickness was also obtained over the width of the intake.

To measure boundary layer thickness, two rakes of pitot tubes were used, one in the position of the outboard edge of the nacelle and the other at the inboard edge. The distances from the wing surface at which the velocity was 0.99 of the local stream velocity were found to be:-

inboard 0.358 inch
outboard 0.130 inch

and these were taken as the values of boundary layer thickness. Scaling for positions between those measured in terms of streamwise distance from the wing leading edge, a cross section profile of the boundary layer in this plane has been drawn in Fig.5. The letters A, B, C on this figure are referred to in section 4.3.3.

The wing flow was surveyed in a plane normal to the surface, using a rake of yawmeters. A typical yawmeter head is shown in Fig.6. With these

instruments, sidewash and upwash angles and pitot pressure could be measured. Distribution of sidewash is shown in Fig.7, plotted as lines of constant outflow angle. This angle is measured parallel to the intake lip and is quoted relative to free stream direction. The mean outflow is of the order of $1\frac{1}{2}^{\circ}$ which indicates that relative to the toe in angle of the nacelle of 2° 46' there is a flow component from outboard to inboard.

Upwash distribution is shown similarly plotted in Fig.8. Upwash angle is measured in a direction normal to sidewash, and is quoted relative to the local wing surface direction on the intake centre line.

The yawmeter heads were physically large relative to the wing boundary layer thickness and therefore upwash angles given by those instruments situated within the boundary layer are in error and have been ignored in the drawing of Fig.8.

The distribution of Mach number is shown in Fig.9. The mean entry Mach number at the outboard intake is 1.935 and at the inboard intake 1.955.

4 RESULTS

4.1 Preliminary experiments

As the intake external shock geometry could not be observed by optical methods, preliminary experiments were made to establish firstly, the critical ramp angle and secondly, throttle settings for critical inlet conditions. A static pressure probe was placed on the lip of each intake, on the duct centre line with the holes positioned about 0.08 inch upstream of the lip. By this means it was hoped to detect the passage of the normal shock as it detached from the intake lip.

To determine critical ramp angles, the throttles were opened wide and the compression surfaces were elevated. The variation of lip static pressure ratio, p_L/P_∞, with ramp angle, ε_3, is shown in Fig.10. For each duct, lip static pressure remains constant as ε_3 increases until a point is reached at which a sudden rise takes place; the value of ε_3 at this point is defined as the critical ramp angle.

Critical values of ε_3 of 15° for the outboard duct and 15.8° for the inboard duct are noted. The difference in these values results from the rather higher mean entry Mach number at the inboard duct. These tests were

made with a value of h/δ of 1.08 and are therefore comparable with those of Ref.1. In Ref.1 the maximum compression surface angle which could be achieved before internal choking occurred was estimated and agreed well with experimental observations. This curve is shown in Fig.11 together with the present critical values of ε_3, which are seen to be 1° to $1\frac{1}{2}^\circ$ greater than the results of Ref.1. However in the present tests, the compression resulting from the chamfer on the inside surfaces of the end walls had been removed, transition of the boundary layer on the compression surface and end walls was not fixed artificially and the test value of Reynolds number was higher, all of which, as discussed in Ref.1, would lead to higher critical values of ε_3. The critical values of ε_3 having thus been established, the remainder of the tests were made with the compression surfaces in these positions.

The characteristics of each individual duct and its effect on its neighbour were obtained simultaneously. This was done by throttling the outboard duct, whilst the inboard throttle was set to obtain critical flow conditions in that duct and then repeating vice versa. The operating points of the intake were observed by means of the lip static pressures and thus, duct flow surveys could be made appropriately. The variations of lip static pressure with mass flow ratio are shown in Fig.12a for both ducts when the outboard throttle is varied and Fig.12b when the inboard throttle is varied. Thus for each case, both the intake critical point (the point at which the terminal shock just detaches from the cowl lip) and the available margin of mass flow without interference* could be established. For the throttled duct, the lip static pressures evidently mark the passage of a normal shock as the ratio p_L/P_∞ rises from a supersonic value to a subsonic value as throttling takes place. In each case this rise begins at values of mass flow ratio between 0.98 and 0.99. For the unthrottled duct, the point at which the pressure rise, due to throttling the other, begins (marking the interference margin) is well defined but the rate of rise is smaller.

---

*In the present context, interference is defined as any effect on the flow, nominally set to critical conditions, in one duct caused by variation of flow in the other duct.

4.2 Measurement and reduction of results

Model systems and instrumentation were as described in section 2.3 of Ref.1 and the main duct flow control and measurement units were as shown in Fig.9 of that report.

Briefly, the flow was controlled by a conical throttle which traversed into the duct exit, thus varying exit area. The flow was surveyed by a rotatable rake of twelve pitot tubes across a diameter. The six tubes on each radial arm were located at the centres of equal area annuli. Four static holes were located around the wall of the duct close to the plane of the pitot tubes and the pressures measured by these were used in association with the pitot pressures. Quoted values of pressure recovery (P_f/P_∞) are the mass flow weighted mean of pressures measured by 72 pitot tubes (6 rake rotational positions × 12 tubes) and referred to free stream total pressure.

Four additional static holes were located around the duct wall further downstream and the pressures measured by these holes, together with an assumption of sonic exit flow, provided the means of deriving the main duct mass flow ratio, A_{∞_f}/A_{en}. The duct exits were, in fact, not calibrated and discharge coefficients of 1.0 have been applied. Throat bleed mass flow ratio, A_{∞_b}/A_{en}, was measured by pitot tubes and static holes in the bleed duct and was controlled by variation of exit area. Inlet mass flow ratio, A_∞/A_{en}, is the sum of the main duct and throat bleed flows.

Transient pressures were measured by transducers housed in the "engine bullets". The transducer outputs were measured by mirror galvanometers with a frequency range 0 to 500 Hz and recorded using ultra-violet sensitive paper. Values of P_A/P_∞ quoted are peak-to-peak amplitudes of the pressure fluctuations referred to free stream total pressure.

4.3 Intake performance

4.3.1 General

The main intake performance and "interference" characteristics are summarised in Figs.13a to d. On these graphs main duct pressure recovery peak-to-peak amplitude of pressure fluctuations when transient flow occurs in the main duct and bleed duct mass flow ratio are plotted as a function of the total inlet mass flow ratio, for all the test values of h/δ. At each

value of h/δ, the performance of each duct is given as they are separately throttled and also, the effects on the inboard duct of throttling the outboard and vice versa. The variations of distortion parameter D_v, with inlet mass flow ratio for an h/δ value of 1.08, are included in Fig.13a.

This information together with data concerning velocity distributions at the measuring stations are summarised, compared with the data of Ref.1 and discussed below under the separate headings of (1) pressure recovery, mass flow and flow condition, (2) the effects of immersion of the intake into the wing boundary layer and (3) interference between ducts.

4.3.2 Pressure recovery, mass flow and flow condition

When the intake is raised clear of the wing boundary layer ($h/\delta = 1.08$), Fig.13a shows peak measured values of pressure recovery to be 0.929 for the inboard duct and 0.924 for the outboard. Peak values of pressure recovery obtained in Ref.1 at values of throat bleed flow similar to the present tests are shown in Fig.14. These are plotted as a function of Mach number for various values of ε_3 and the two points for the present tests are included on the graph. The result for the inboard duct aligns well with the previous results but the point for the outboard duct is a little low. It is surprising that the outboard duct, whose mean entry Mach number is 1.935, has a lower peak recovery than the inboard whose mean entry Mach number is 1.955. The more non-uniform sidewash and upwash distributions for the outboard duct may be responsible.

The maximum values of mass flow ratio measured in the two ducts are similar and approximately unity. These are close to maximum estimated values which are indicated on Fig.13a. The estimated values are obtained by assuming isentropic compression from a free stream Mach number of 2.0 to the local entry Mach number (1.955 inboard, 1.935 outboard), with a further shock compression produced by a 7° wedge. Because of the uncertainty of setting the nacelle relative to the wing in a pitch sense (see section 2.2) and because of the local upwash (Fig.8), the estimated maximum values of A_∞/A_{en} could vary by ± 0.01 about the values shown in Fig.13a. The measured maximum mass flow ratios are much closer to the estimated values than those of Ref.1. This may be due to reduced spillage at the sidewalls (because of the reduced leading edge angle) and the increased Reynolds number of the present test.

It was demonstrated in Ref.1 that when a duct was throttled, a point was reached (often not far subcritical) at which a high frequency (≈400 Hz) generally low amplitude pressure fluctuation occurred in the duct. On further throttling, a second point was reached at which a low frequency (≈60 Hz) oscillation of much larger amplitude started. In the present tests, Fig.13a shows that similar characteristics appear in the inboard duct with high frequency oscillation starting at $A_\infty/A_{en} = 0.82$ and low frequency oscillation at A_∞/A_{en} at 0.64. In the outboard duct however the high frequency oscillation is completely absent and the low frequency oscillation occurs at $A_\infty/A_{en} = 0.87$.

The flow distortion parameter D_v $\left(= \frac{V_{max} - V_{min}}{V_{mean}} \text{ at any given radius}\right)$ is plotted against duct radius in Fig.15. Points are also included from Fig.31 of Ref.1 and these are interpolated with respect to stream Mach number but the implied values of ε_3 are somewhat lower than those of the present tests. The worst distortion occurs at $r/R \simeq 0.9$ and the variation of D_v at $r/R = 0.88$ with mass flow ratio is included, for each duct, in Fig.13a.

4.3.3 Effect of immersion of intake into wing boundary layer

Because of transverse curvature of the under surface of the wing, the boundary layer thickness profile in the region of the intake is correspondingly curved. In order to define the degree of immersion of the straight leading edges of the compression surfaces into this curved prifile, points A and B (Fig.5) were used for the measurement of h and the intake was always immersed so that $h_A = h_B$. On this definition of h, when $h/\delta = 0.75$ the point C (Fig.5) was just at the edge of the boundary layer.

Intake performance characteristics for various values of h/δ are shown in Fig.13. To summarise the effects of immersion into the wing boundary layer, some of these quantities are plotted as a fraction of h/δ in Fig.16.

In general intake performance does not suffer significantly from immersion into the boundary layer to a value of h/δ of 0.75. Indeed, small gains in recovery are noted, the peak values in both ducts with $h/\delta = 0.75$ being between ½% and 1% greater than with $h/\delta = 1.08$. Pressure distributions at the measuring station are shown for these two cases in Fig.17. They are

seen to be very similar with no significant region of lower pressure on the compression surface side for the case with $h/\delta = 0.75$ but with some increase in the area of high pressure. Immersion has little effect on the low frequency instability boundary of the outboard duct (Fig.16) and only a small effect on the inboard. D_v (at $r/R = 0.88$) worsens slightly with immersion, more so in the inboard duct than the outboard. The additional distortion parameter R_v ($= V_{max}/V_{mean}$), has been included in Fig.16 and is seen to be unaffected in either duct by immersion.

4.3.4 Interference between ducts

As noted earlier interference effects were investigated by setting the throttle of one duct to provide roughly critical intake flow and throttling the other one, whilst surveying the flow in both. With the intake mounted on the wing, this had to be done for both ducts in turn as it was anticipated that non-uniformities in entry flow conditions could give rise to asymmetric interference effects.

It was found that similar characteristic curves were obtained in a throttled duct whether it was being throttled in unison with the other or whether it was being throttled individually, with the other running full. Interference data are therefore presented in Fig.13a to d as curves of pressure recovery, throat bleed flow and pressure fluctuation amplitude for the duct running nominally at its critical point condition but plotted as a function of the mass flow ratio in the other (throttled) duct. Numbers adjacent to the recovery curves for the duct which is running at its nominal critical point, show the actual mass flow passing through the duct at that point. Thus, for example, in Fig.13a, the performance of the outboard duct (plotted as a function of the mass flow through the throttle inboard duct) is given in the top right hand graph. The performance of the inboard duct is shown in the top left hand graph.

To summarise interference effects, Fig.18 shows:

Curve A - the mass flow ratio in the throttled duct at which the pressure recovery in the other (unthrottled duct) starts to fall.

Curve B - the mass flow ratio in the throttled duct at which the pressure recovery in the other has fallen by 1%.

Curve C - the mass flow ratio in the throttled duct at which some instability is induced in the other.

From these curves the following margins* are noted at a value of h/δ of 1.0.

	Affected duct - $(1 - A_\infty/A_{en})$	
	Outboard	Inboard
Recovery starts to fall (A)	0.290	0.125
Recovery fallen by 1% (B)	0.440	0.270
Instability induced (C)	0.340	0.195

It is evident from the table that interference margins are considerably lower when the outboard duct is throttled than when the inboard duct is throttled. The wing flow sidewash distribution (Fig.7) indicates that there is a small mean component of the flow from outboard to inboard which may account for these asymmetric effects. Thus it appears that interference effects may be sensitive to small crossflow angles and that interference by the windward duct on the leeward is likely to be more severe** than vice versa.

Another interesting feature shown in the above table is the fact that once the pressure recovery in a duct starts to fall, the rate of decline is similar in each of the two ducts, i.e. the two values of (B - A) are similar.

Interference margins as indicated by the lip static pressures were shown in Fig.11. Comparing these with the appropriate curves of Fig.13a, it is evident that in each case, the lip static pressure starts to rise at

---

*The term "margin" is the amount of spillage $(1 - A_\infty/A_{en})$ which occurs in the throttled duct before a given condition is reached in the other.

**The word "severe" is used with reference to the mass flow margins involved. It does not describe any intensity of interference.

values of A_∞/A_{en} about 2% higher than the values at which the pressure recovery starts to fall.

Although interference margins for throttling the inboard and outboard ducts are somewhat different, namely 0.290 and 0.125, they show the improvement of the current splitter design in preventing interference, over the previous three configurations tested in Ref.1. This is illustrated in Fig.19, in which results for all four splitter configurations are presented, showing the variation of pressure recovery with mass flow ratio, each from a condition of maximum recovery and mass flow.

Thus, by carrying a splitter extension around the cowl lip so as to cover the region of shock confluence, interference effects may be reduced to an order satisfactory for practical purposes on the present design.

5 CONCLUSIONS

Because of design changes to the model and Reynolds number differences between the present tests and those of Ref.1, the effects of the change in environment, from a uniform flow field to that produced by a slender wing, have not been directly assessed. However peak pressure recovery values measured in the present tests compare well with those of Ref.1, while maximum values of mass flow ratio are rather better.

Immersion of the intake into the wing boundary layer does not degrade its general performance significantly for small amounts of ingested boundary layer and indeed, small improvements in pressure recovery are noted.

Carrying the leading edge of an extended splitter (duct dividing wall) around the cowl lip greatly improves the interference margins. However, these appear to be sensitive to small crossflow angles at the intake and smaller (though still adequate) margins are noted in the case of interference of the windward duct on the leeward, than vice versa.

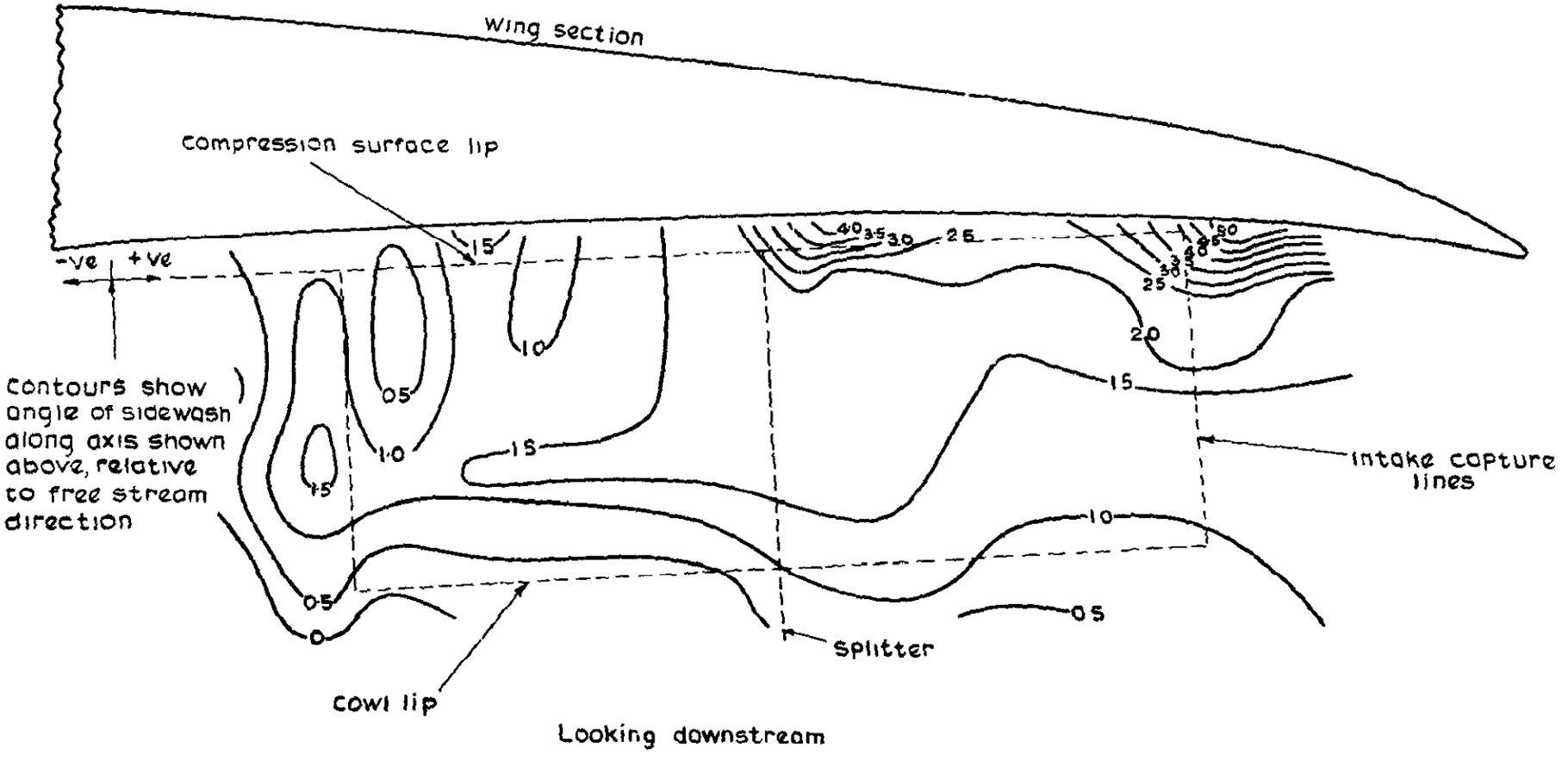

Fig.7 Local wing flow — sidewash distribution
(see section 3 for description)

REFERENCES

No.	Author	Title, etc.
1	M. D. Dobson	Wind tunnel tests on a rectangular, twin duct, variable geometry air intake at supersonic speeds. A.R.C. C.P. 944 (1966)
2	B.A.C.	Supersonic trarsport. Definition of nacelle geometry - prototype and interim engine variants. SST/B72A - 05.3/2047 (1964)

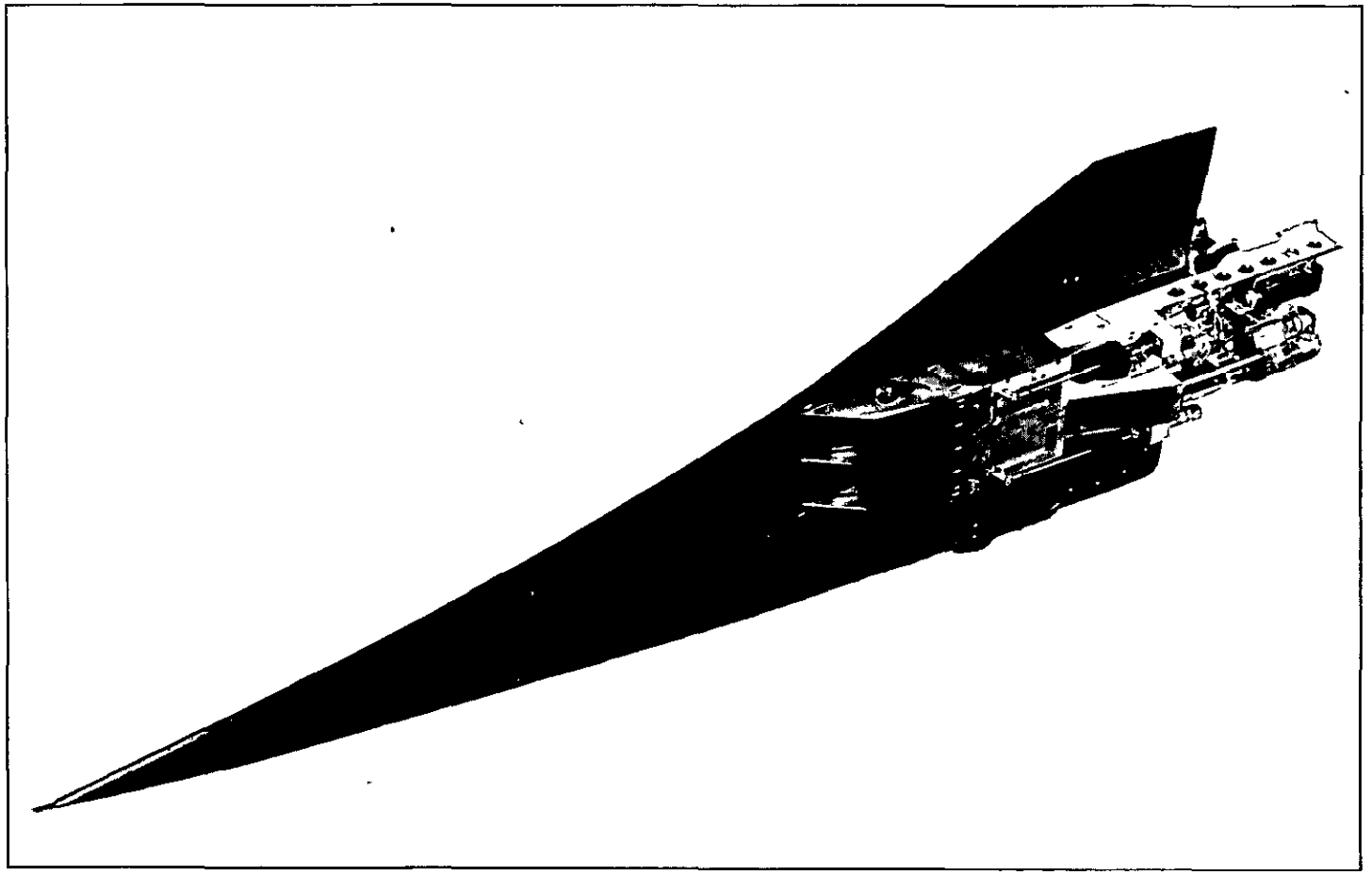

Fig.1. The model

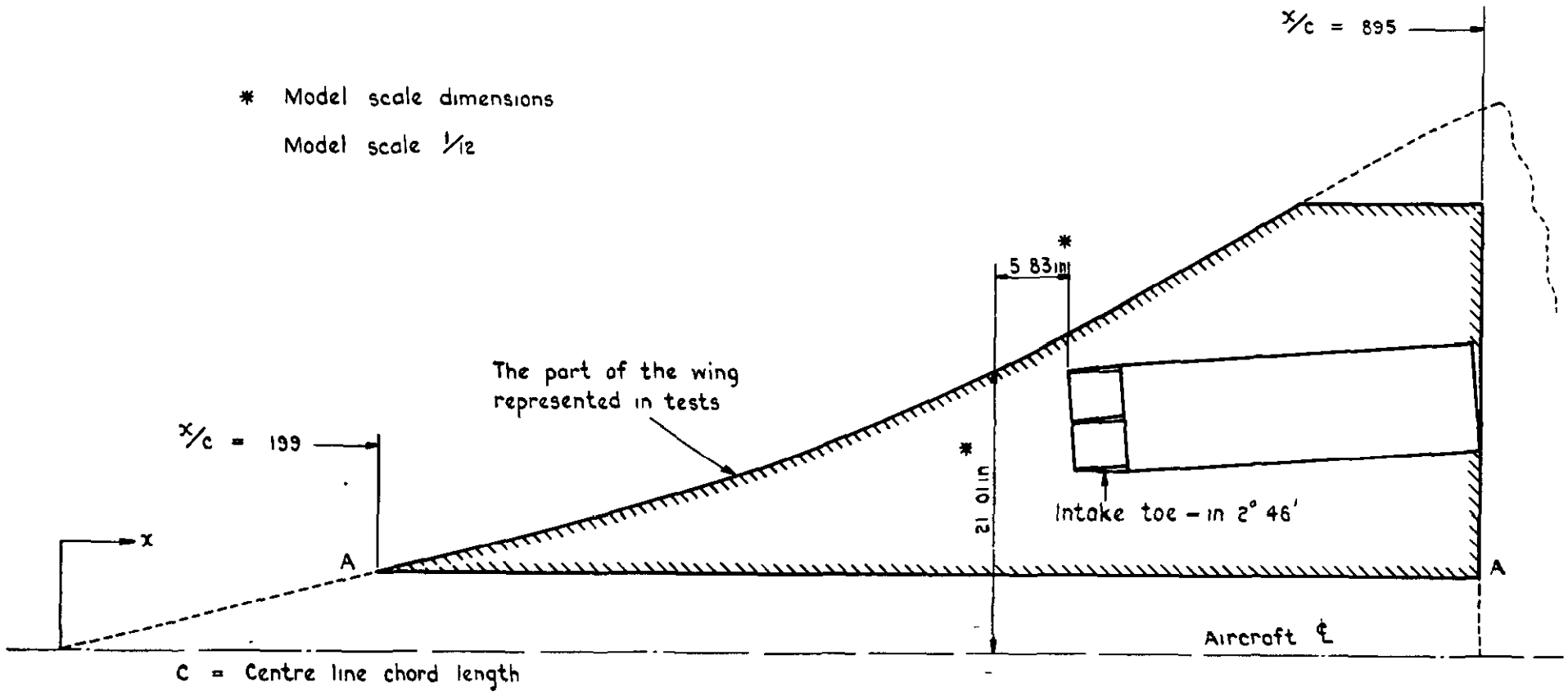

Fig. 2 Sketch showing the part of the wing represented and the location of the nacelle

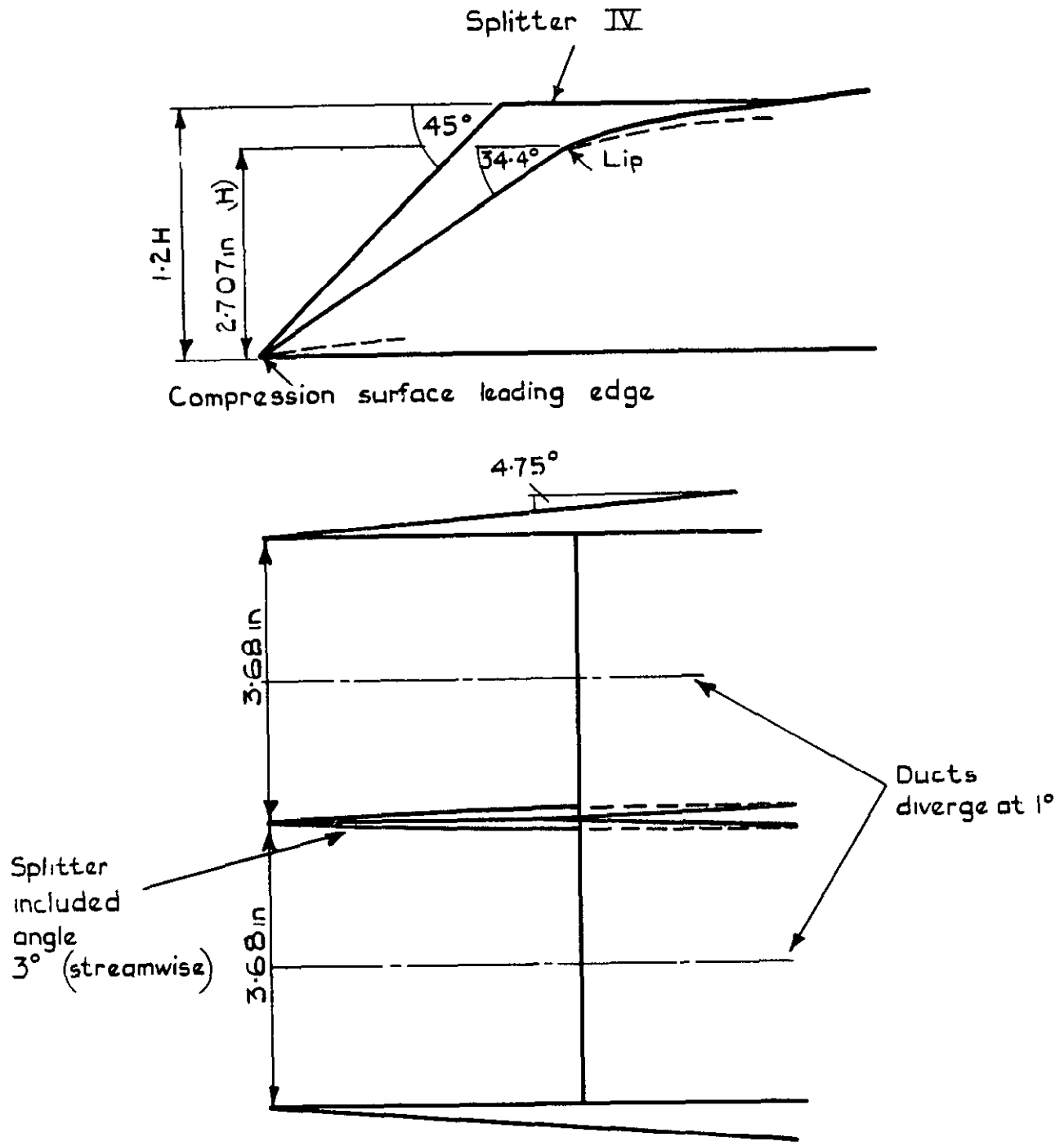

Fig 3 Inlet details

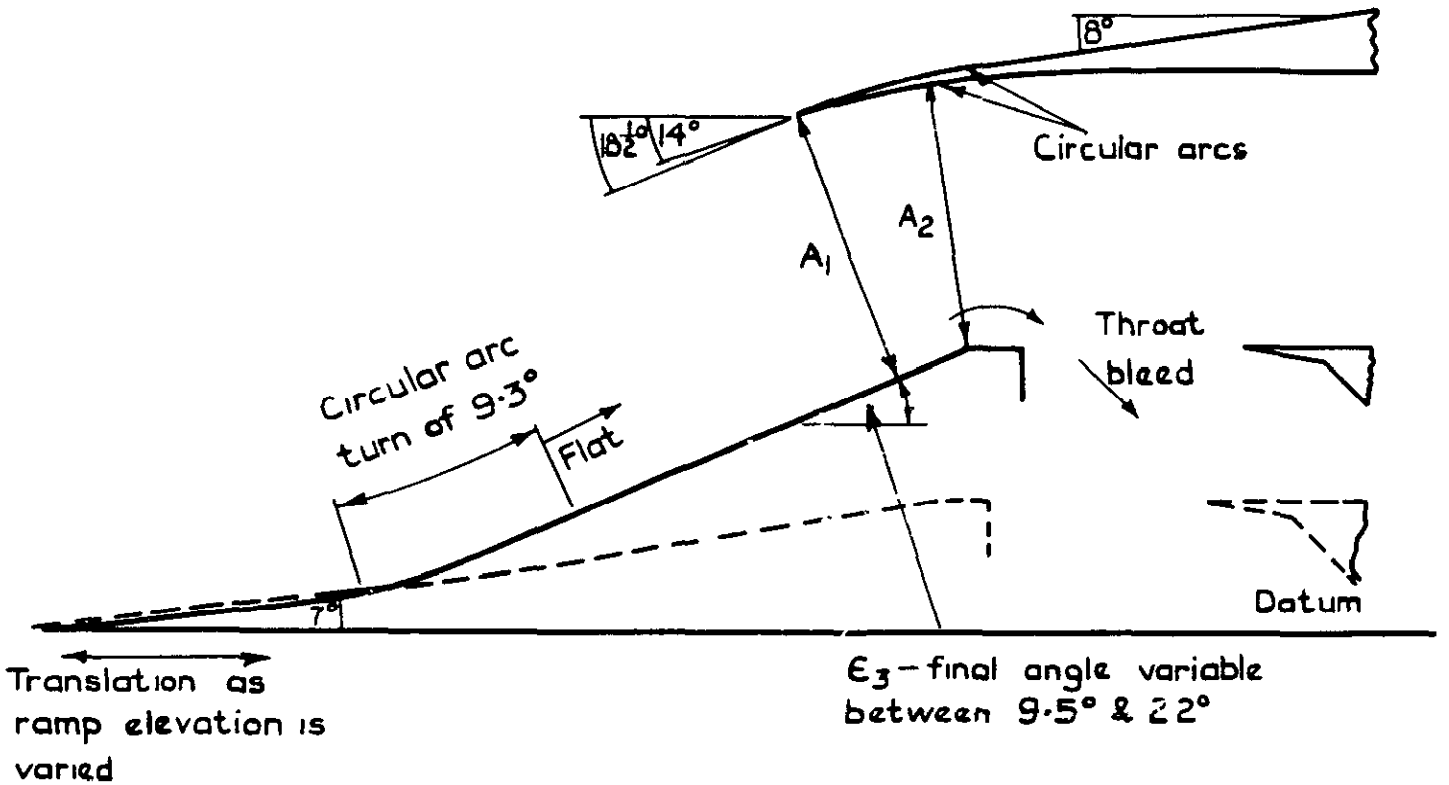

Fig. 4 Compression geometry

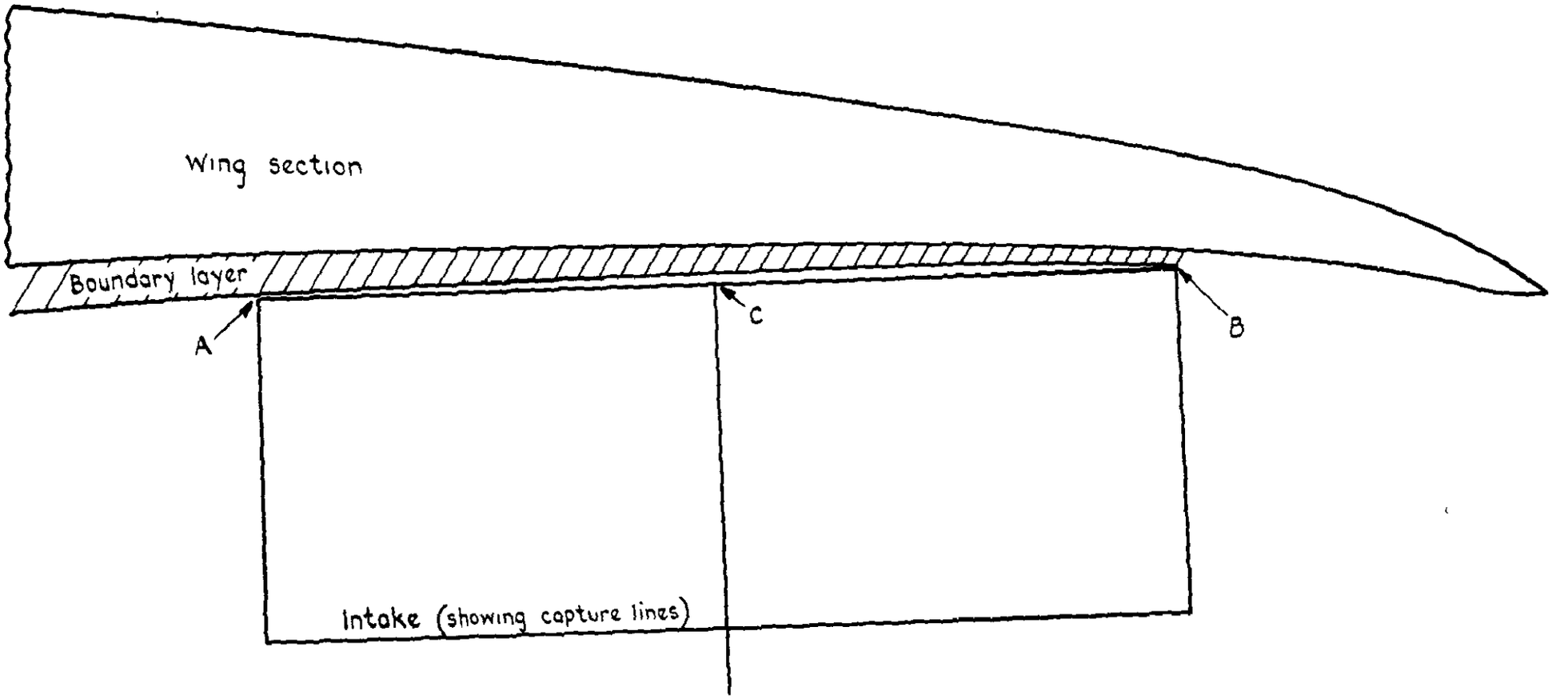

Fig.5 Section at plane of leading edge of compression surface

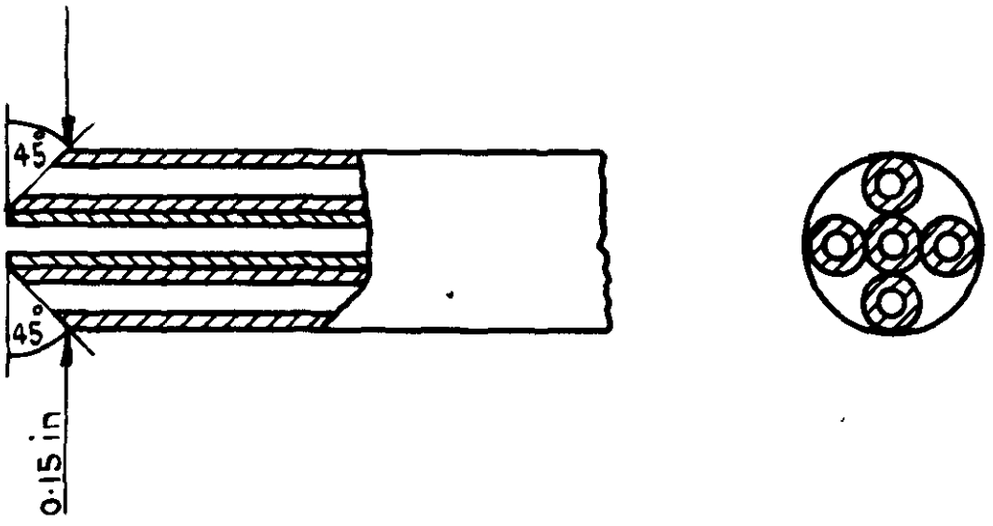

Fig. 6 Typical yawmeter head

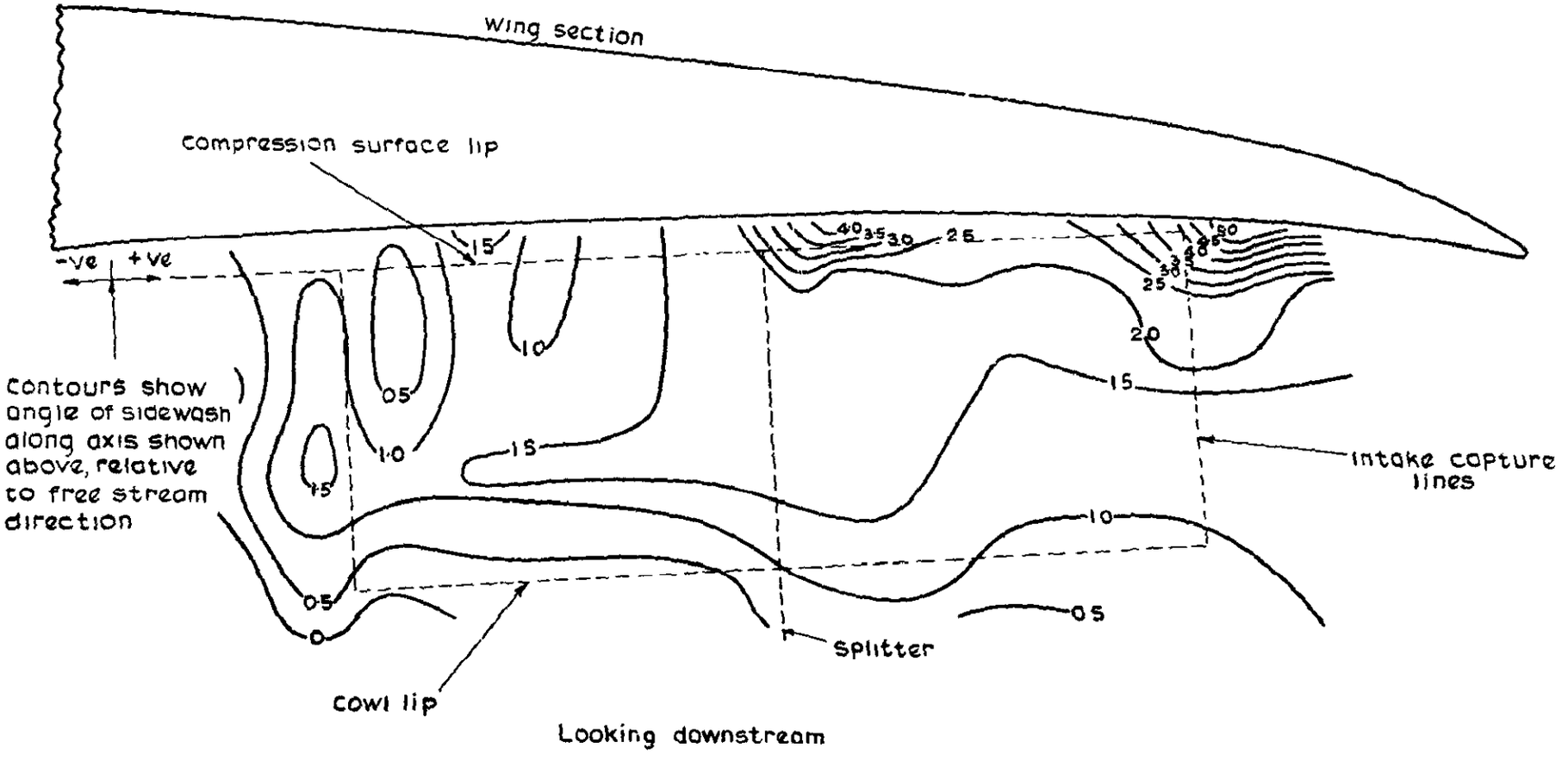

Fig.7 Local wing flow — sidewash distribution
(see section 3 for description)

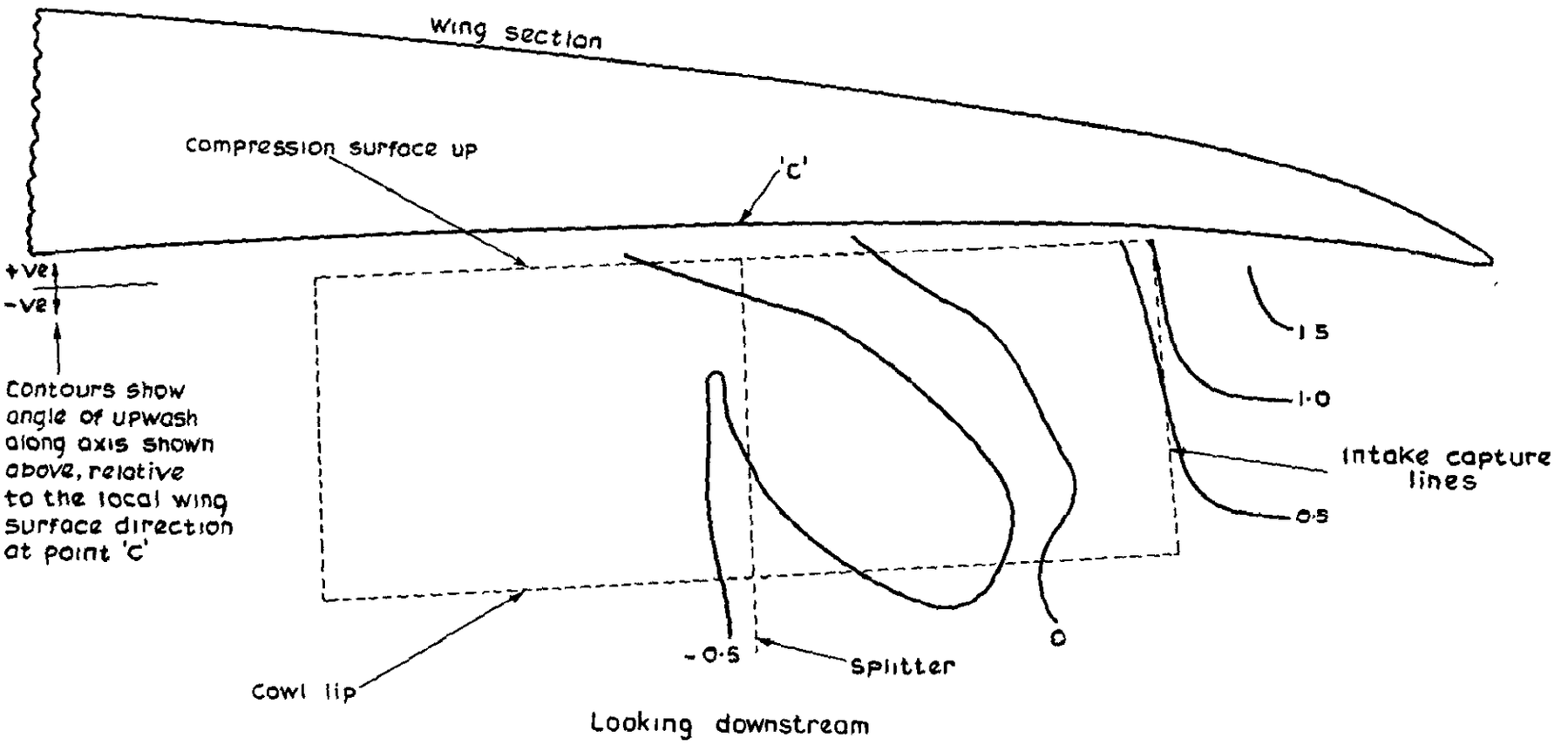

Fig. 8 Local wing flow — upwash distribution
(see section 3 for description)

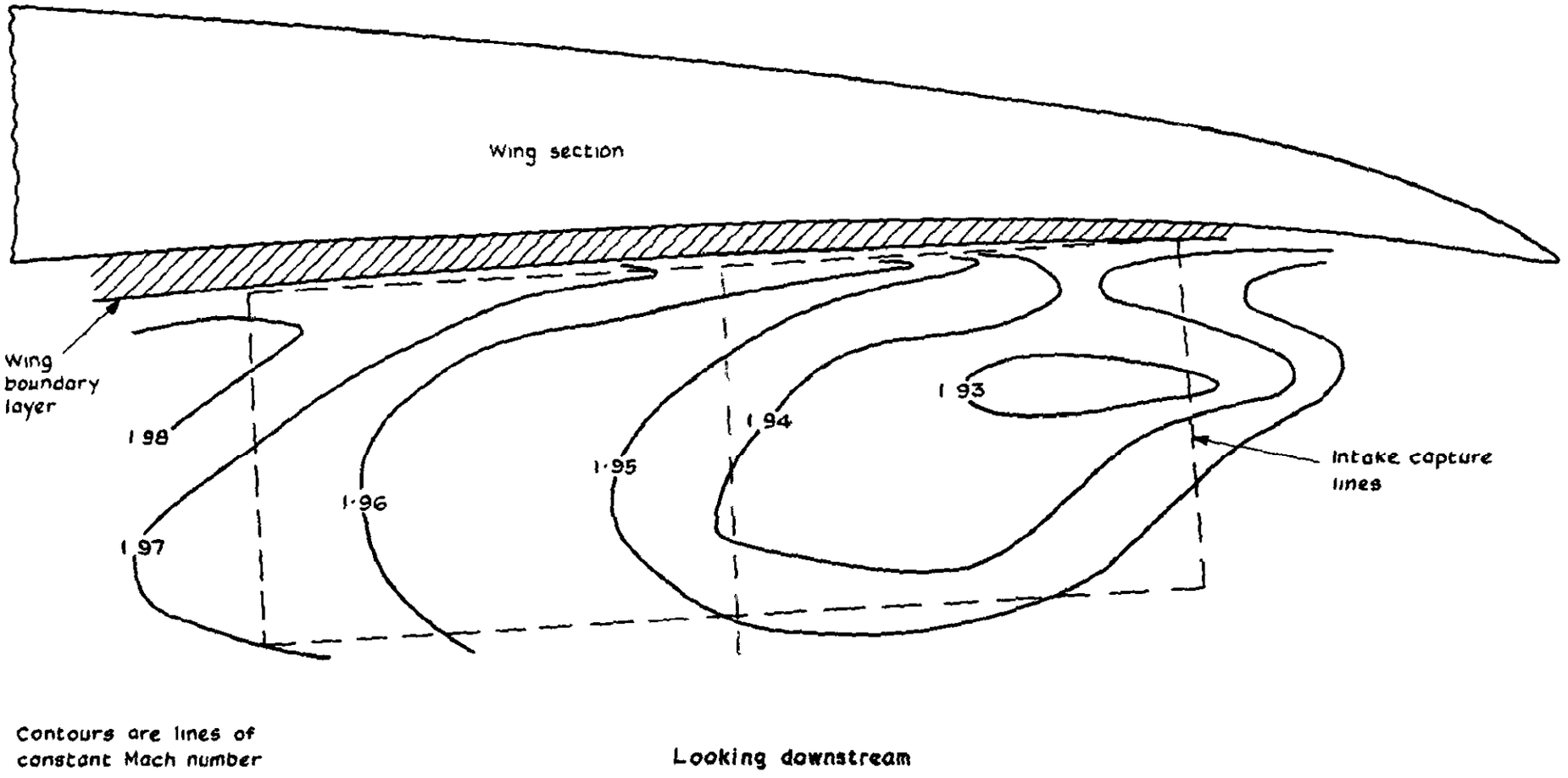

Fig. 9 Local wing flow - Mach number distribution

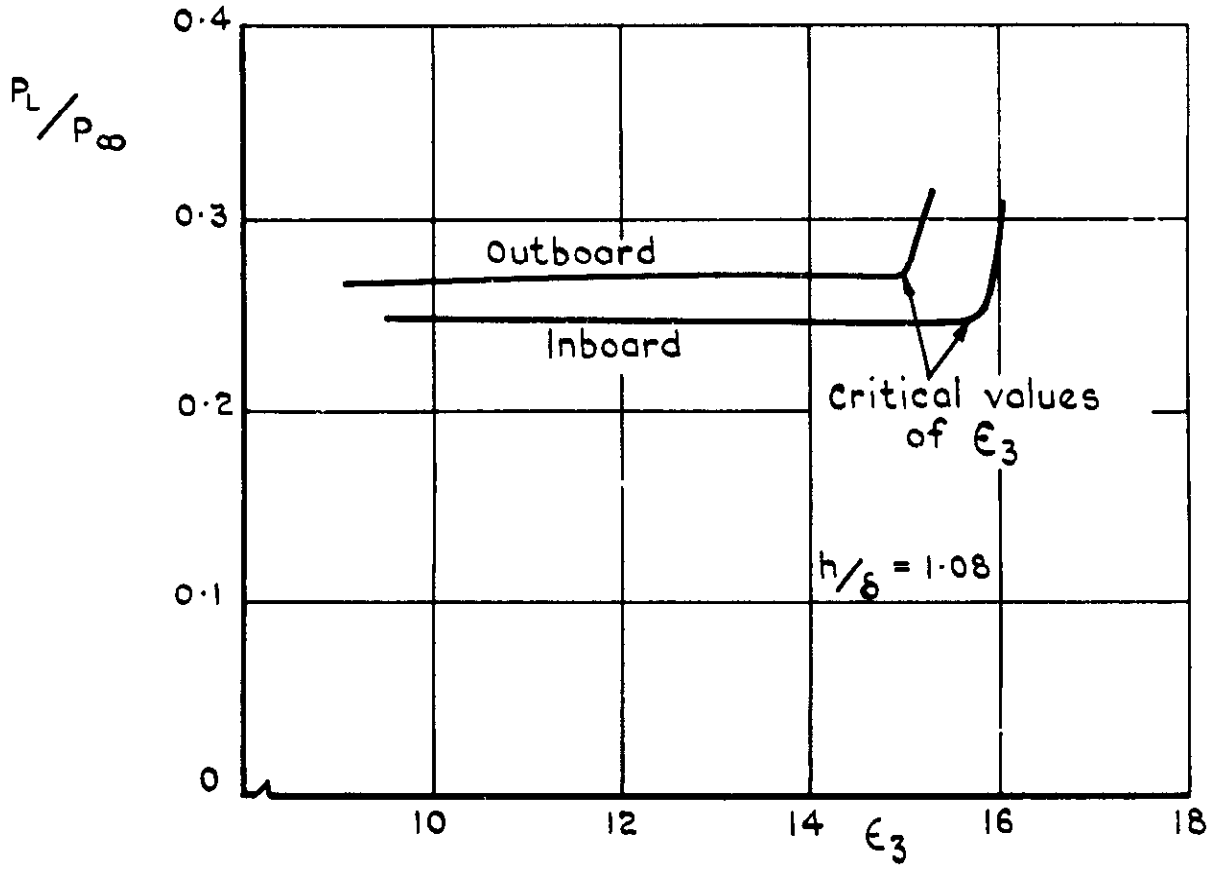

Fig. 10 Lip static pressure – variation with compression surface angle

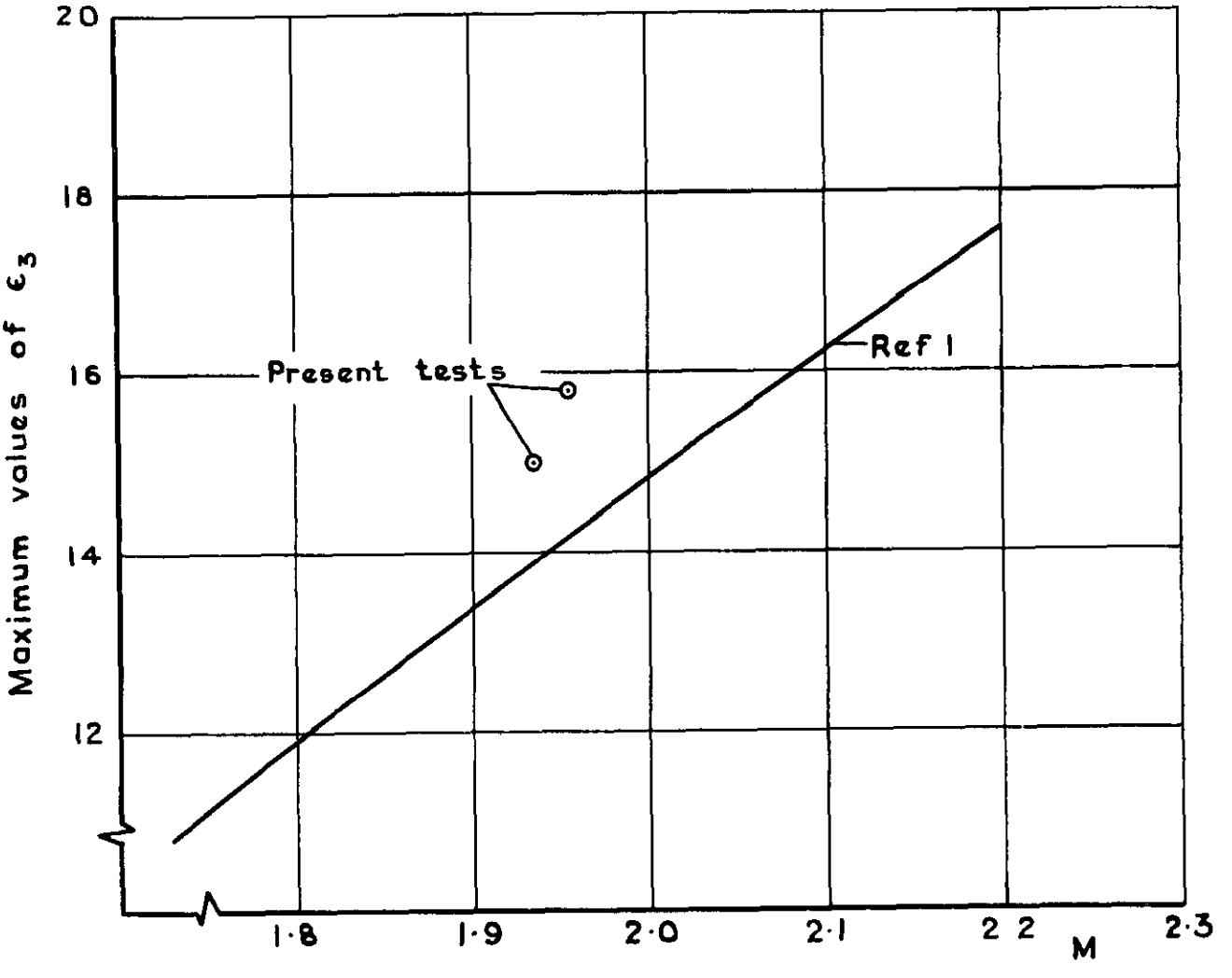

Fig.11 Maximum values of ϵ_3 before choking in the inlet throat occurs — variation with Mach number

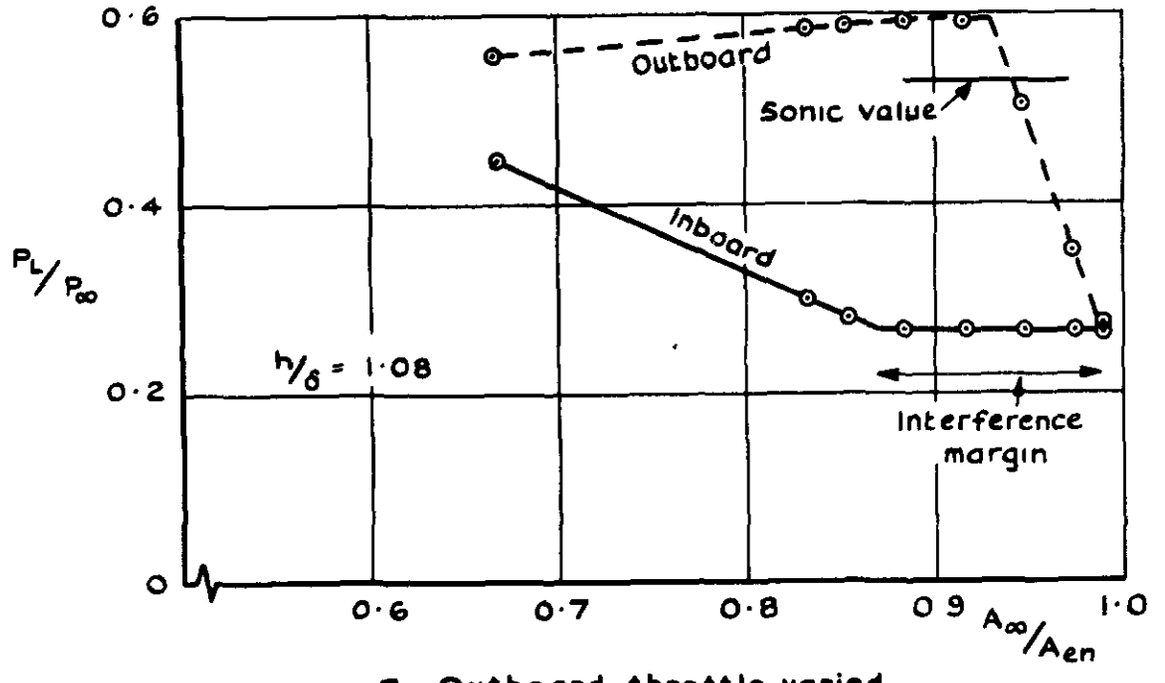

a Outboard throttle varied

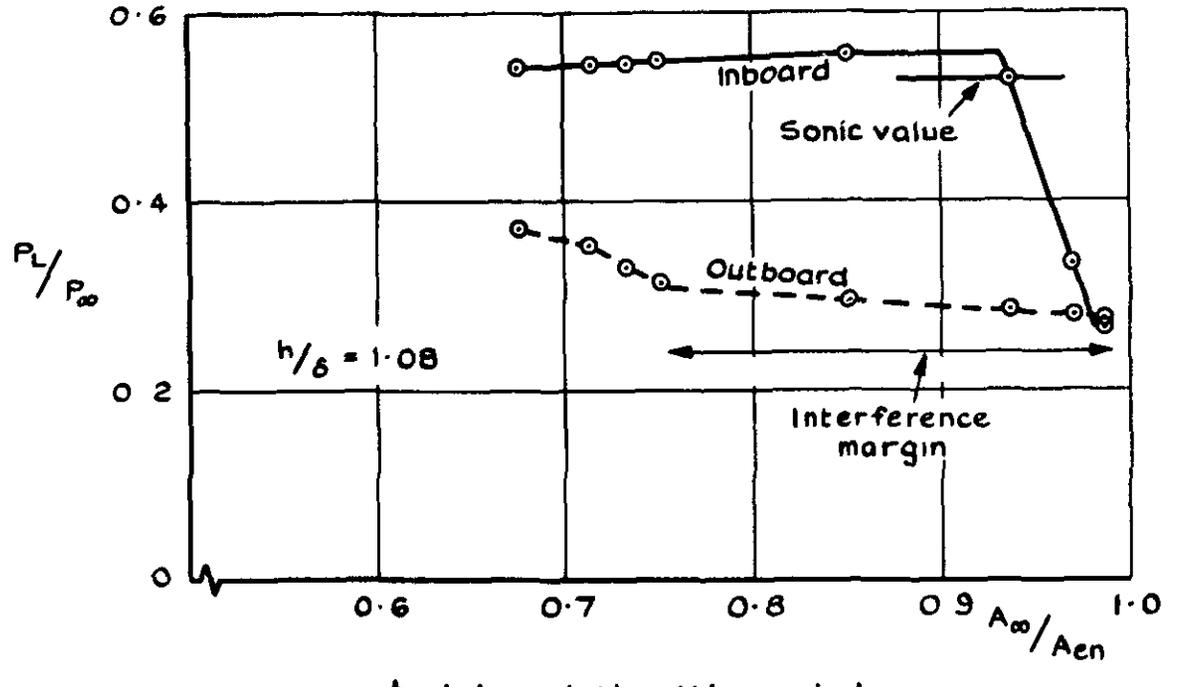

b Inboard throttle varied

Fig. 12 Lip static pressure – variation with mass flow ratio

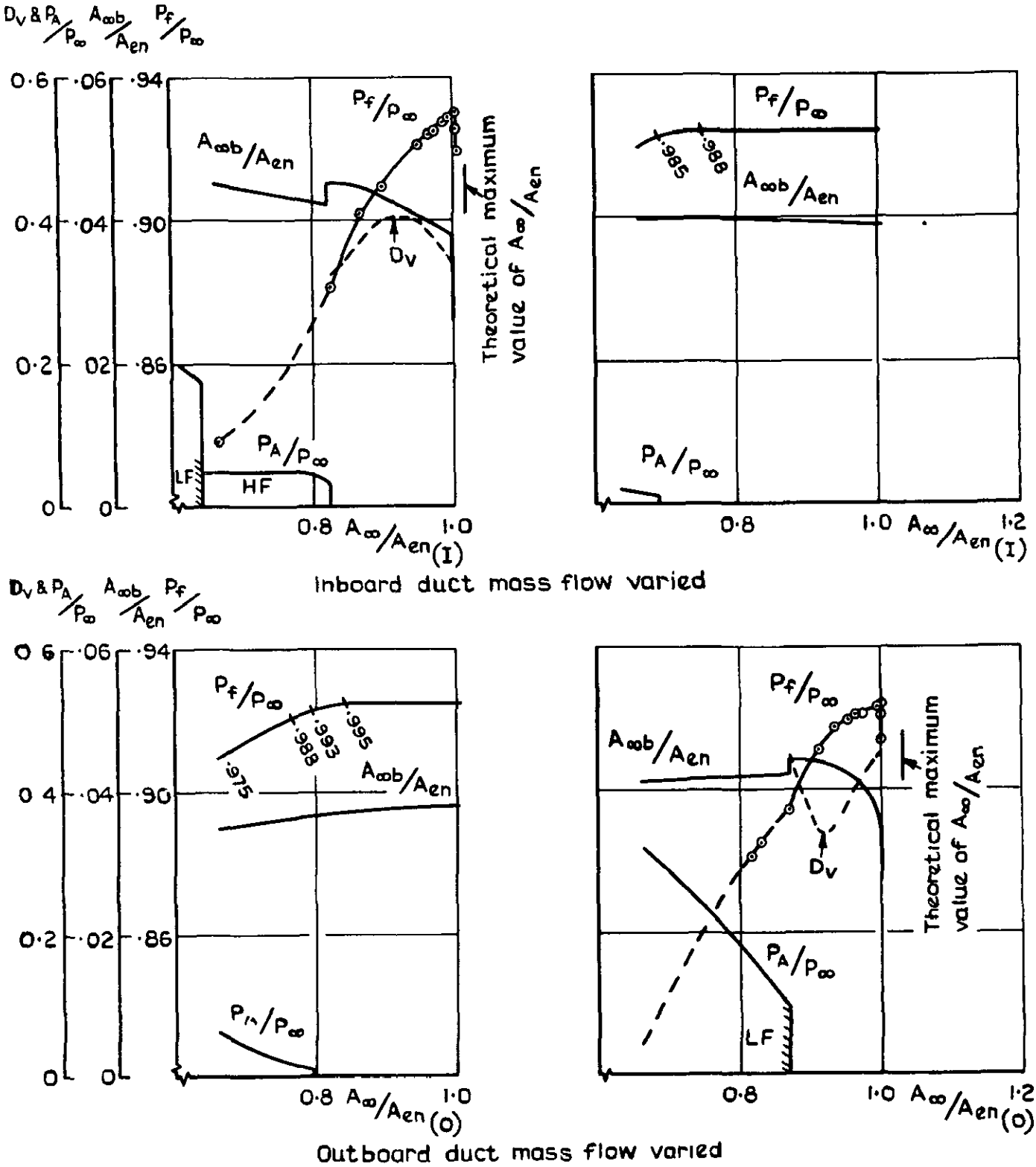

Fig.13 Performance characteristics of intake

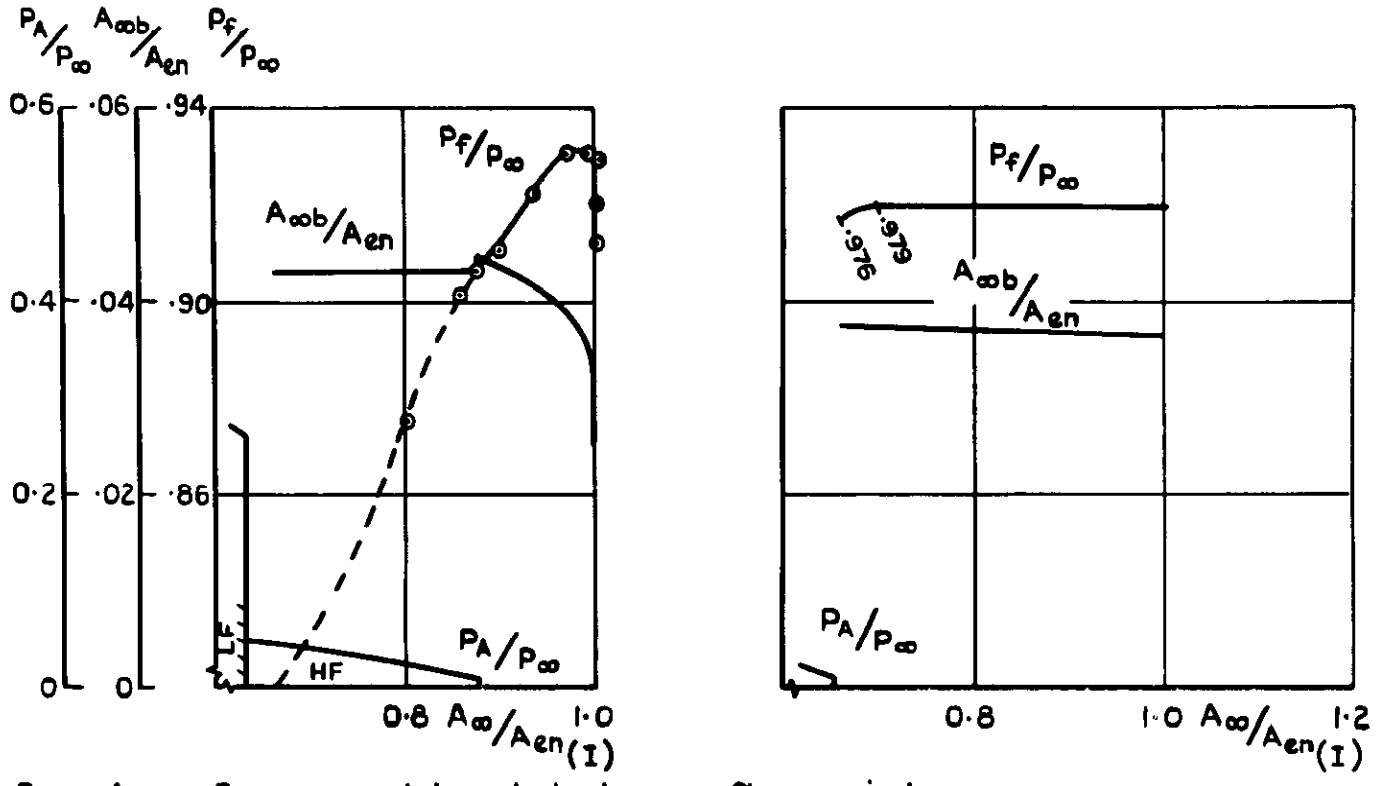

Inboard duct mass flow varied

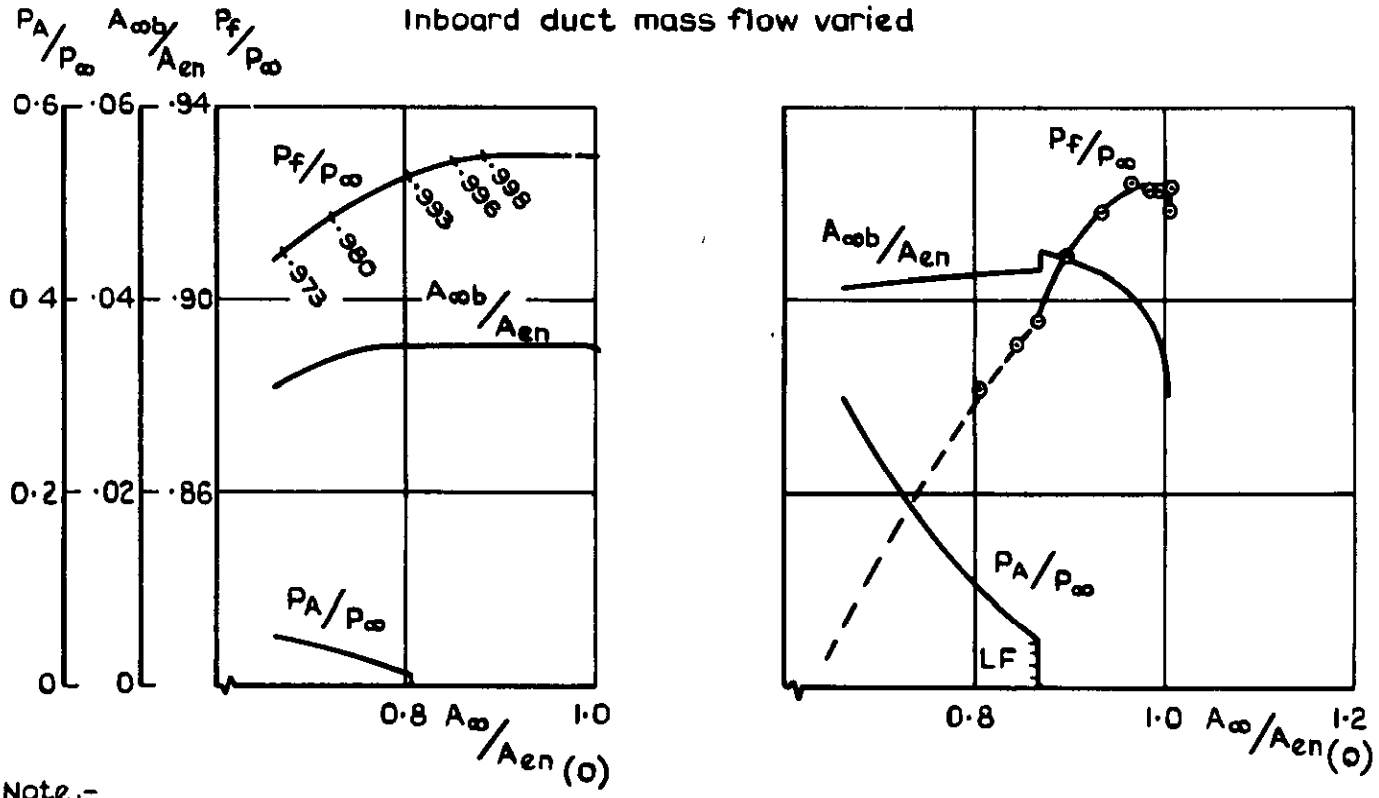

Note.-
Numbers adjacent to curves of P_f/P_∞ show the actual value of A_∞/A_{en} through the duct at that point

Outboard duct mass flow varied

Inboard duct

Outboard duct

b $h/\delta = 0.95$

Fig. 13 contd

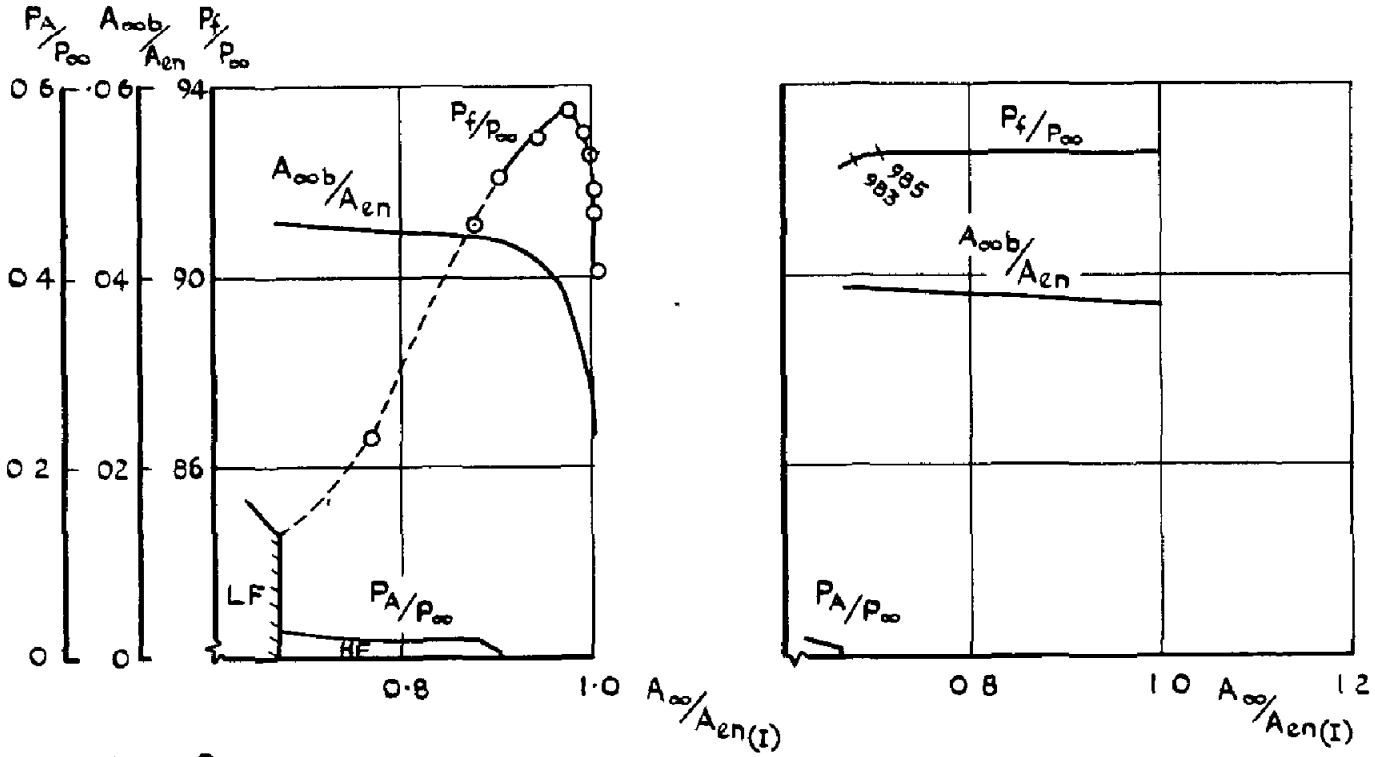

Inboard duct mass flow varied

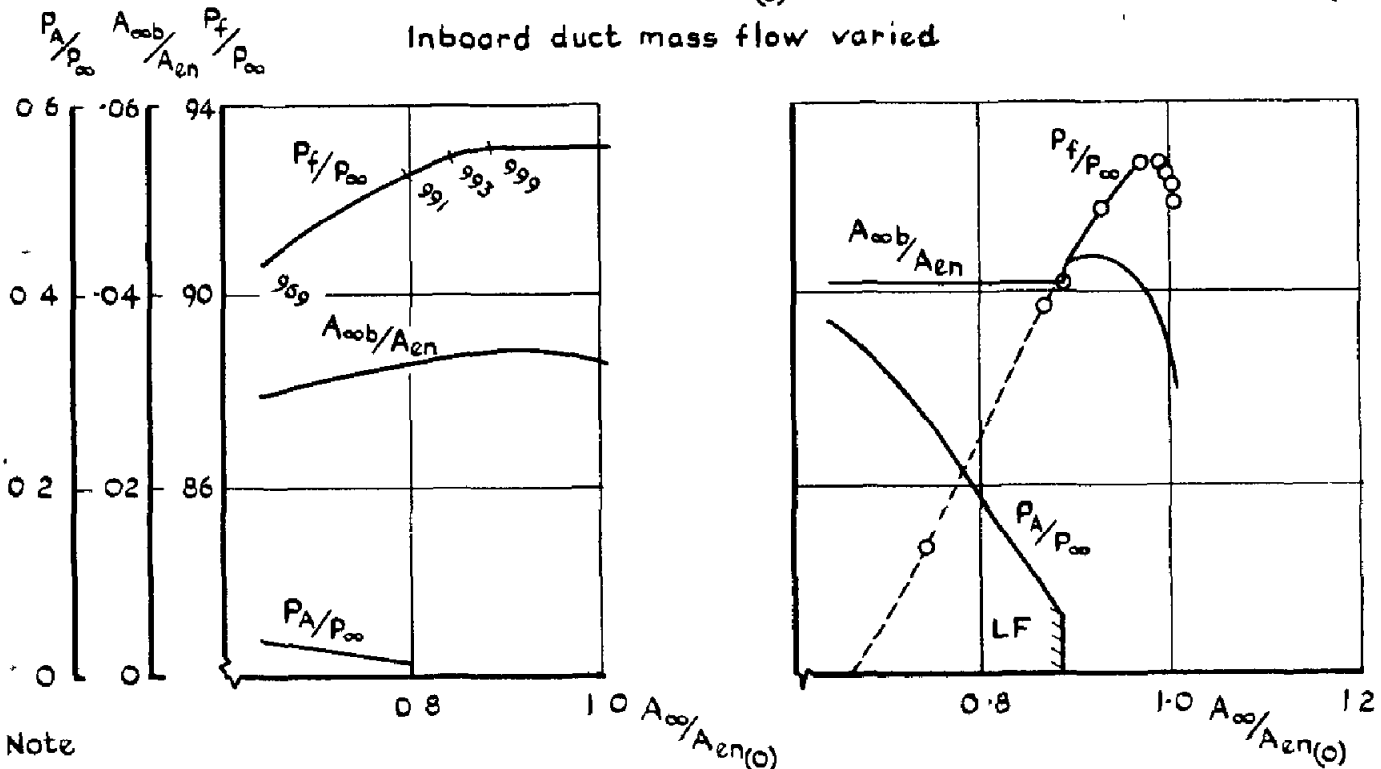

Note
Numbers adjacent to curves of P_f/P_∞ show the actual value of A_∞/A_{en} through the duct at that point

Outboard duct mass flow varied

Inboard duct

Outboard duct

c $h/\delta = 0.83$

Fig 13 contd

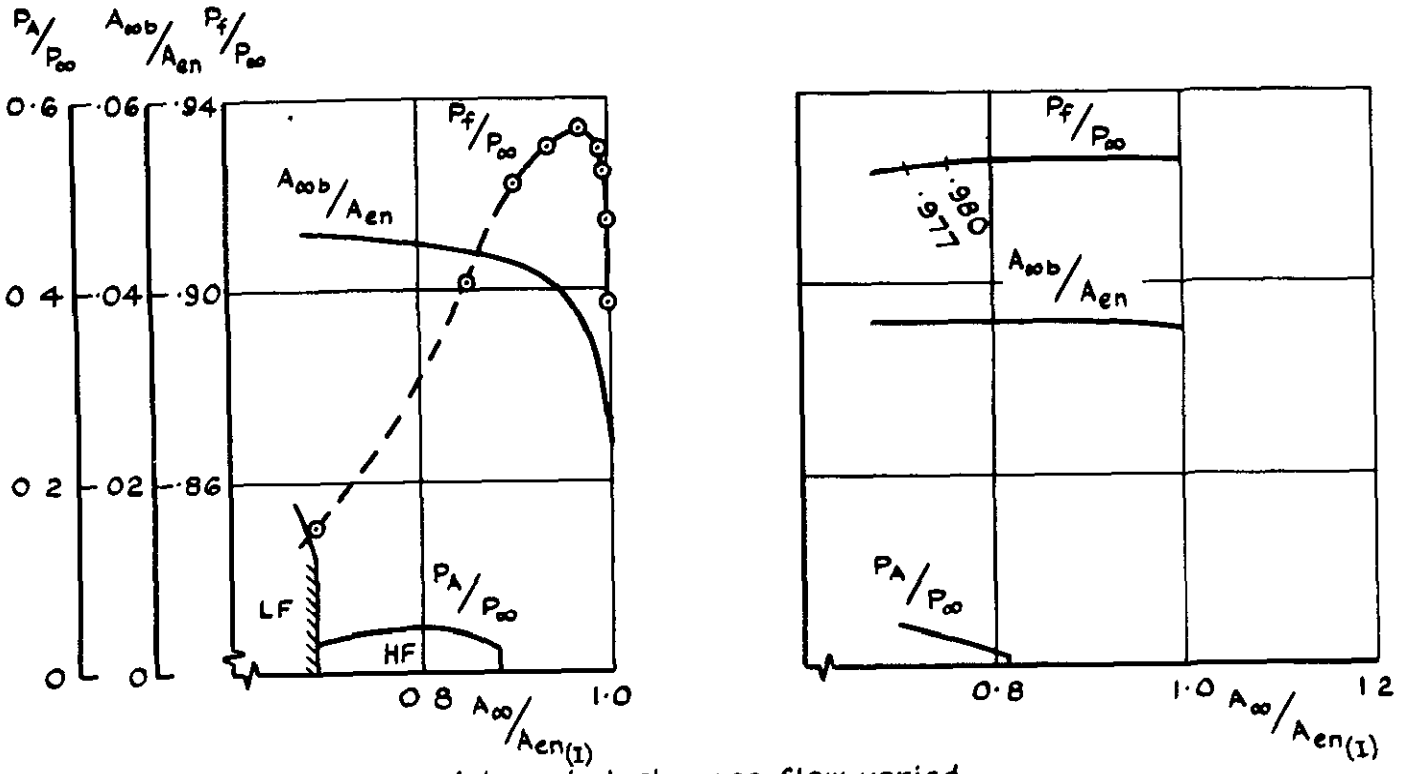

Inboard duct mass flow varied

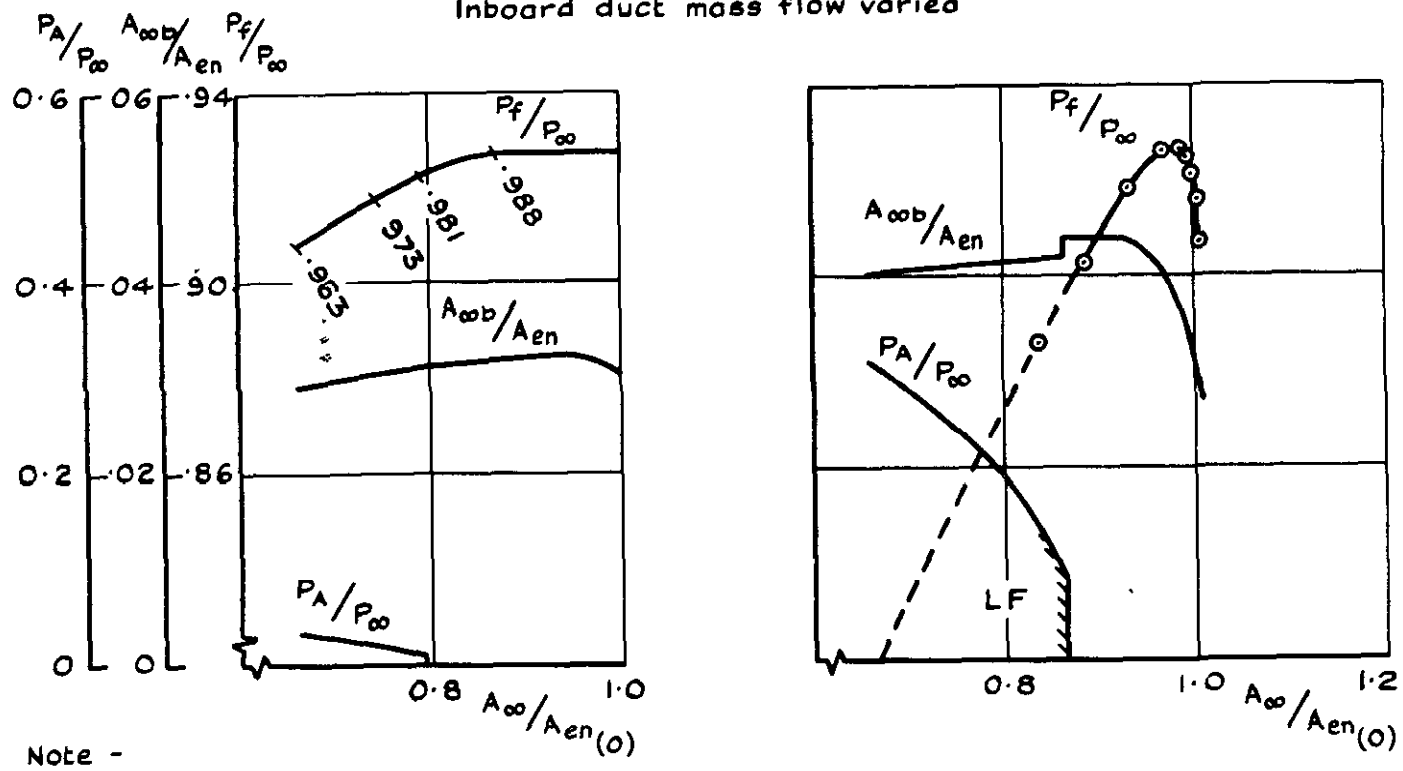

Note -
Numbers adjacent to curves of P_f/P_∞ show the actual value of A_∞/A_{en} through the duct at that point

Outboard duct mass flow varied

Inboard duct

Outboard duct

d $h/\delta = 0 \cdot 75$

Fig. 13 concld

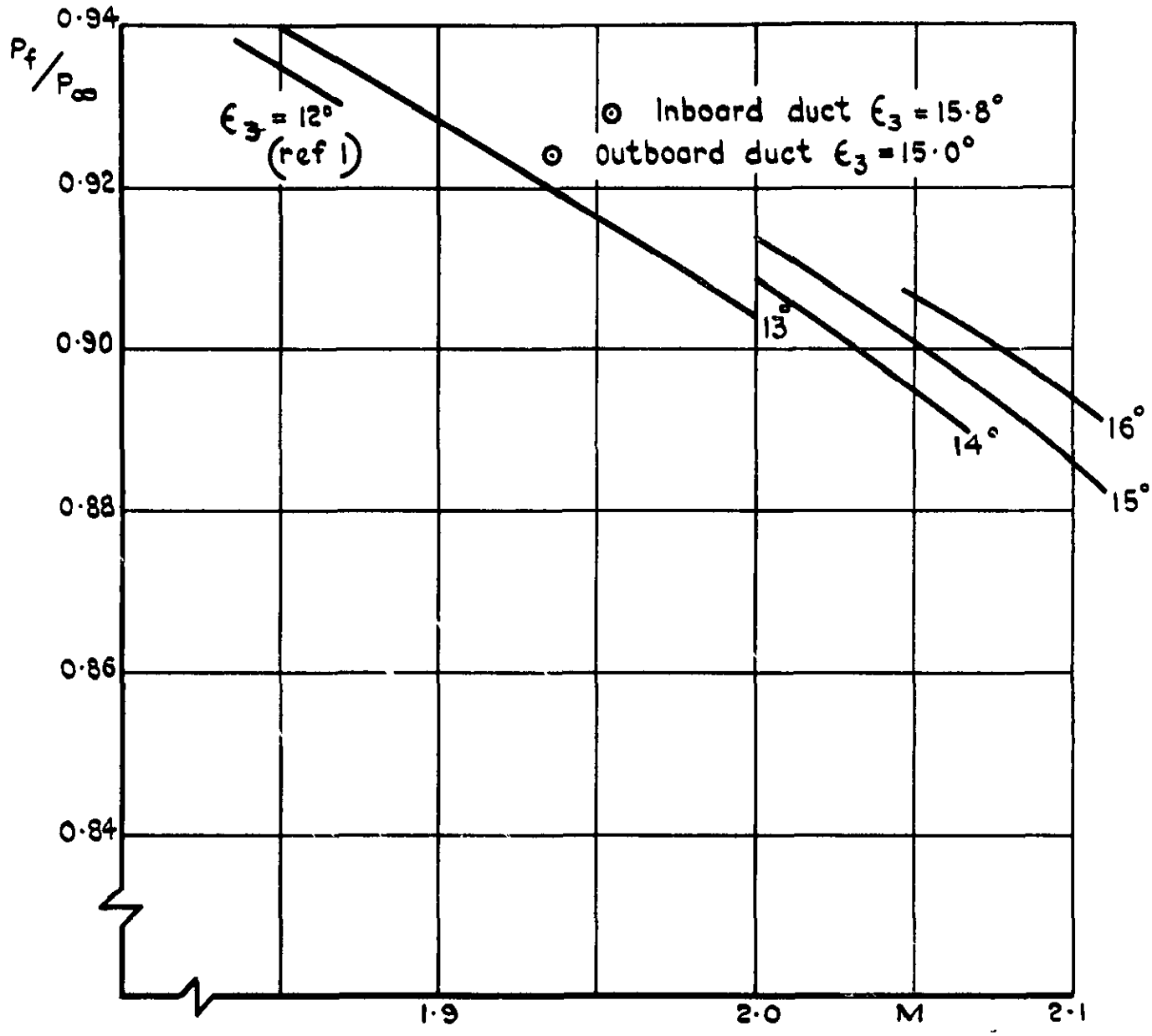

Fig. 14 Peak pressure recovery — variation with inlet Mach number

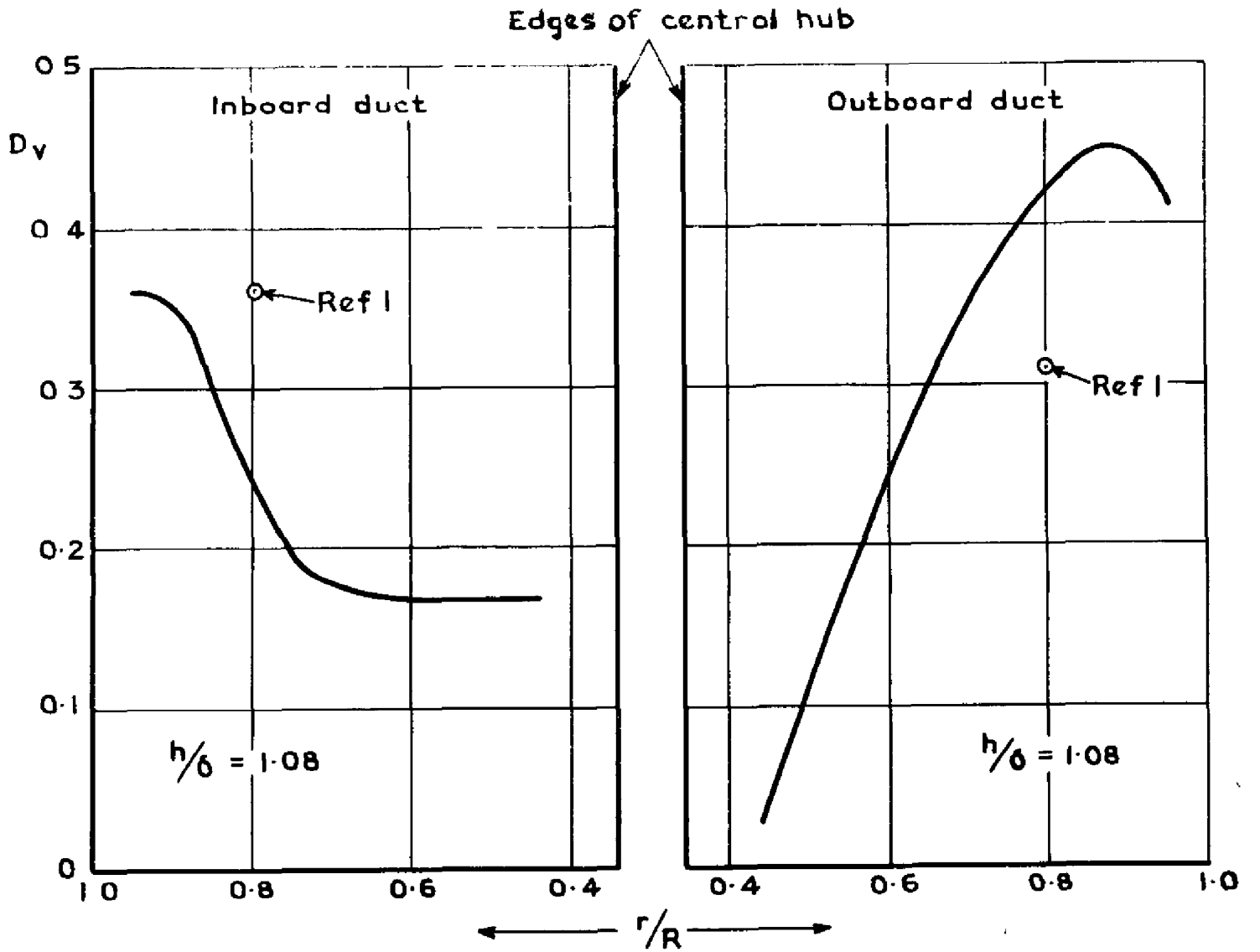

Fig. 15 Distortion parameter D_V — variation with radial position

(Ducts running at peak recovery)

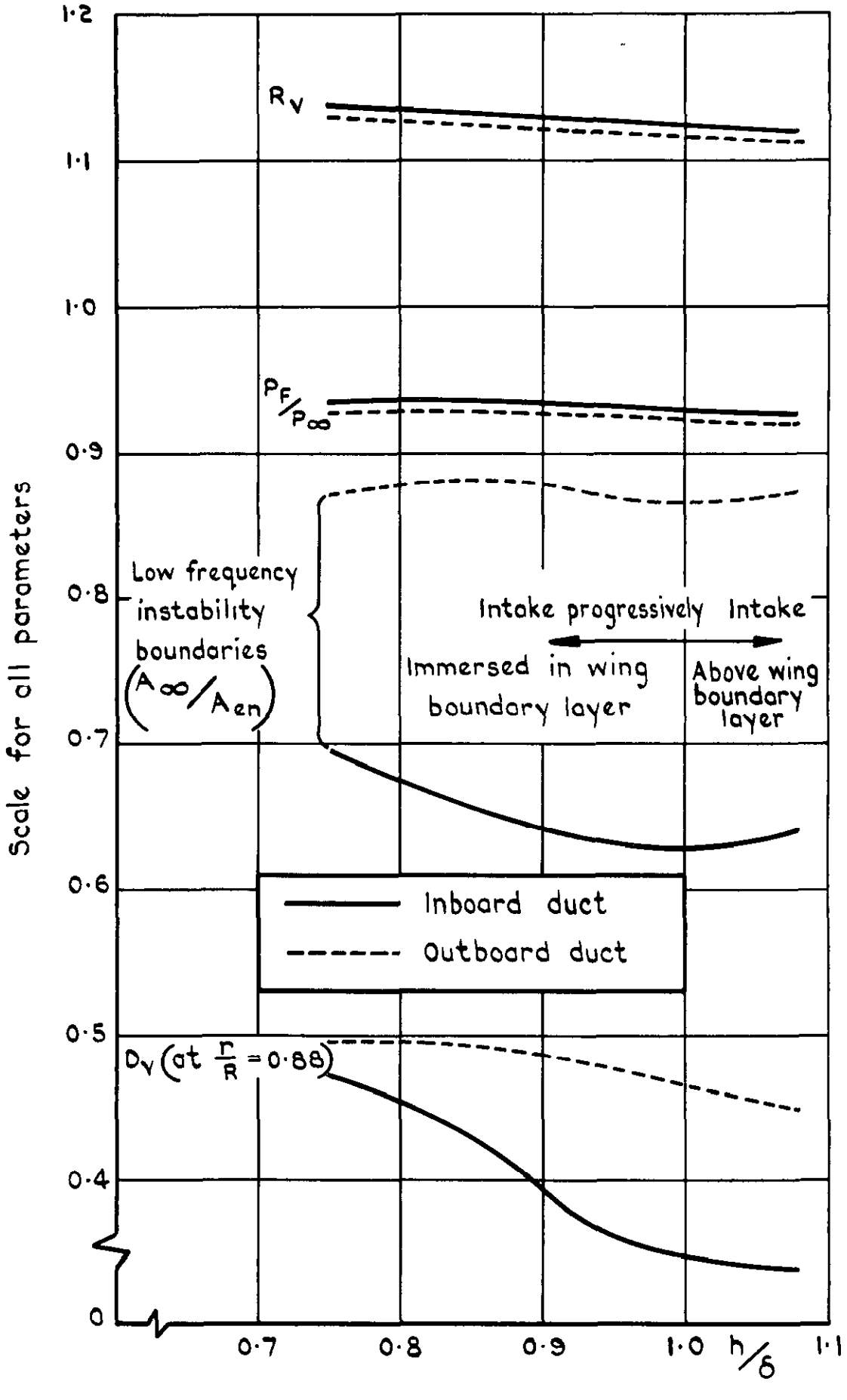

Fig. 16 Effect of immersing intake into wing boundary layer

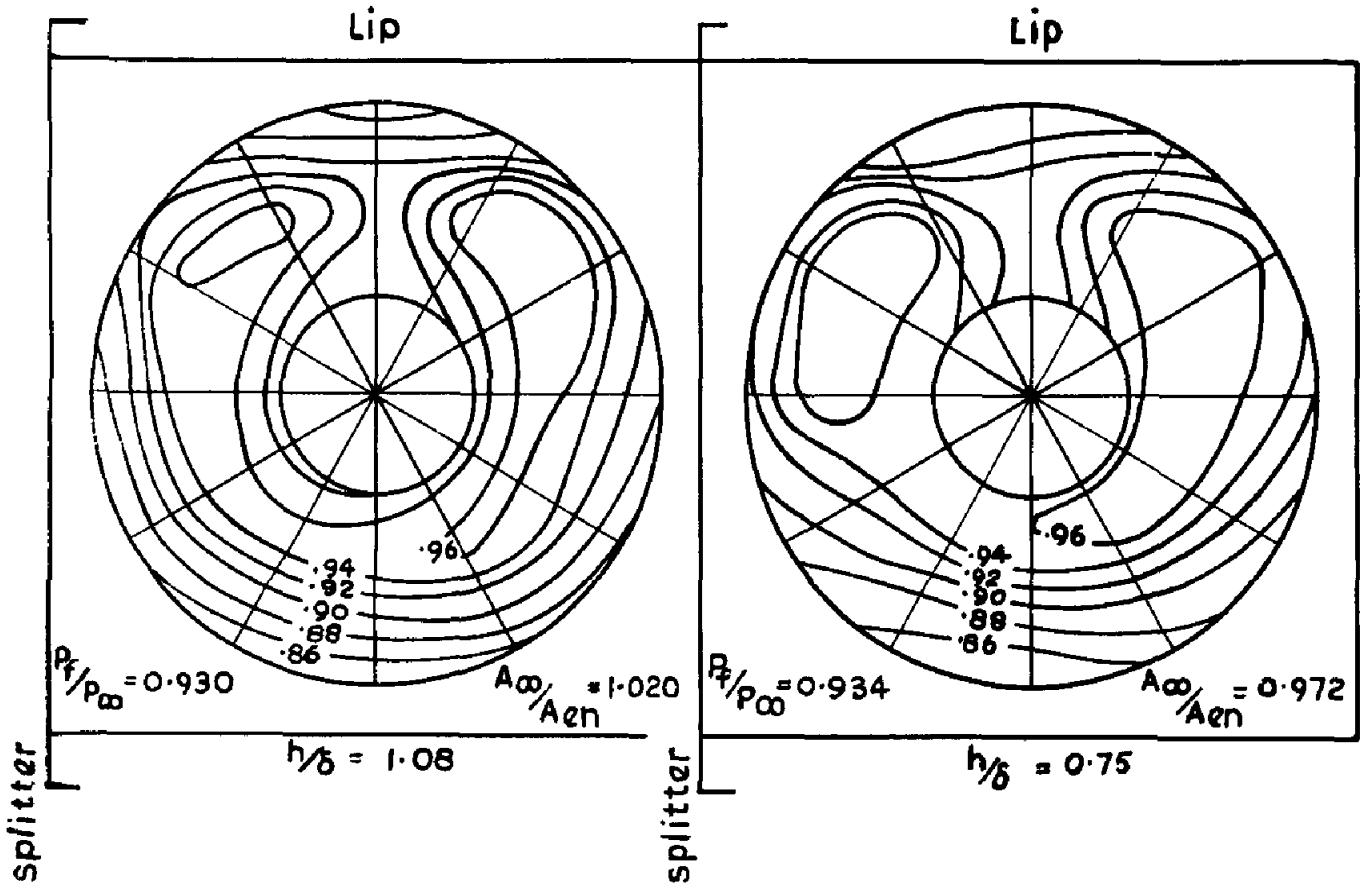

Fig. 17 Pressure distributions in inboard duct at peak recovery

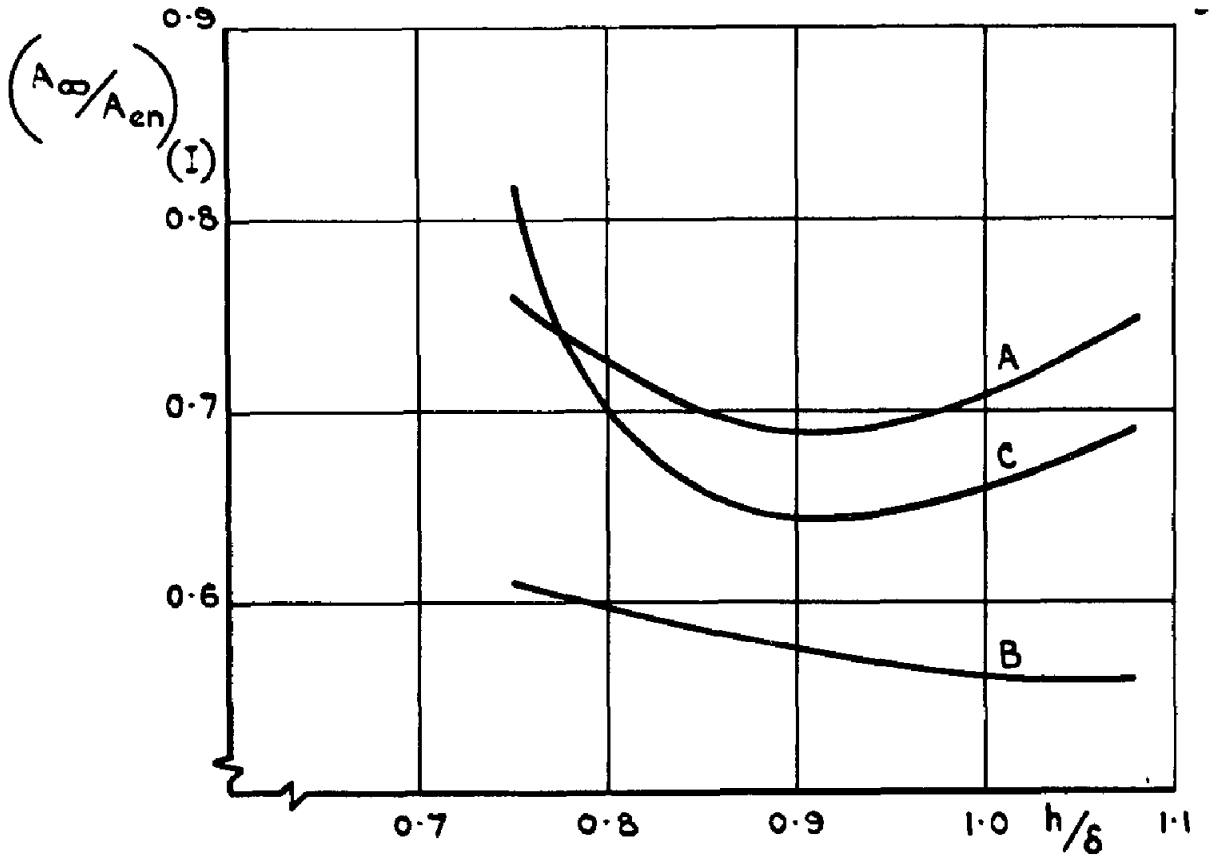

a Effects on outboard duct

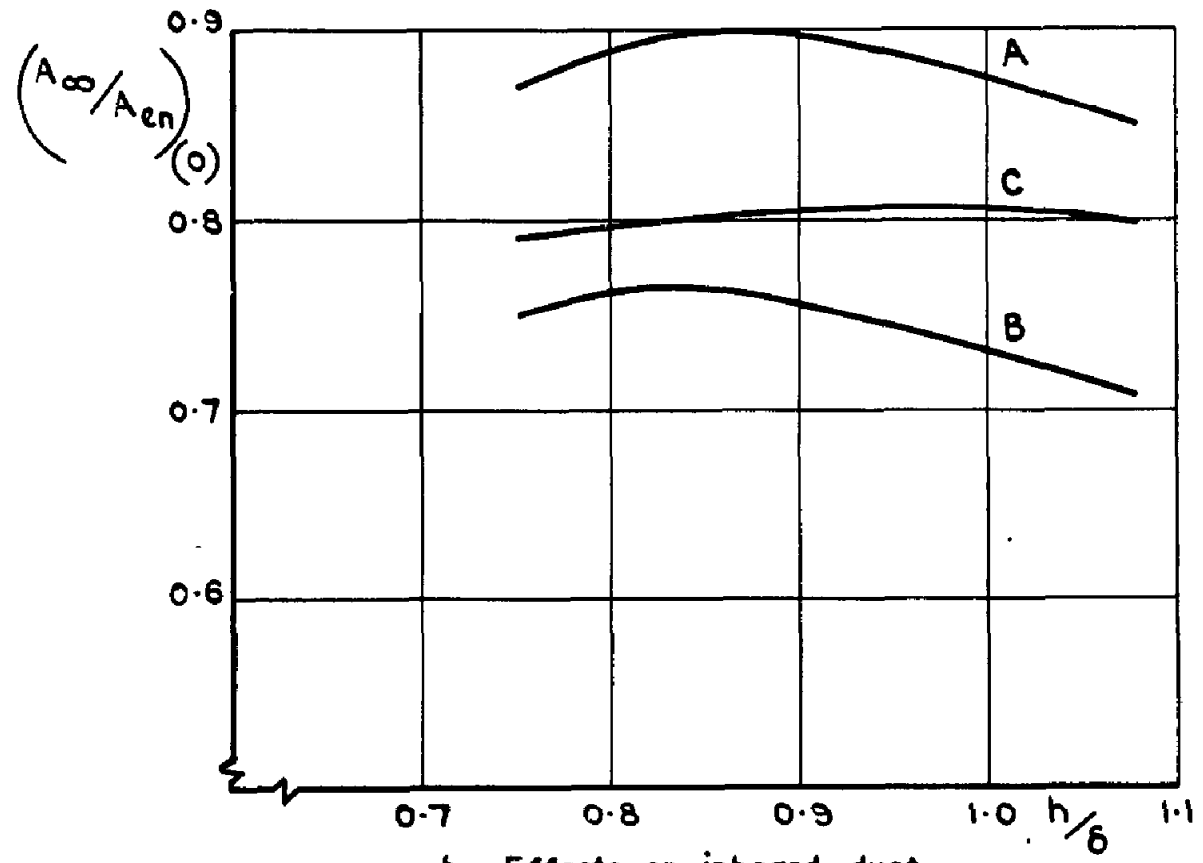

b Effects on inboard duct

(For explanation of lettering A, B, C see section 4.3.4)

Fig. 18 Interference boundaries – variation with h/δ

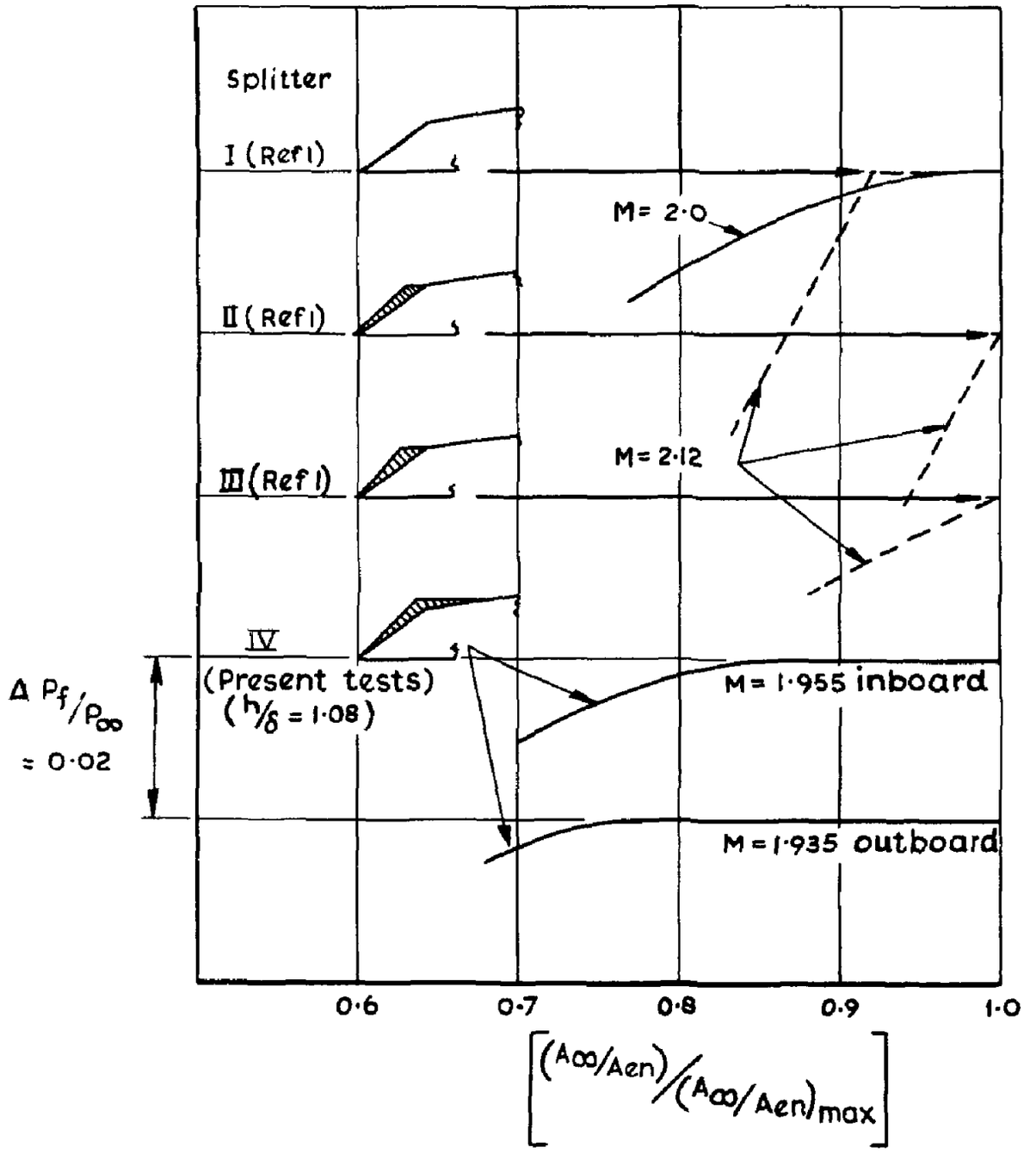

Fig.19 Effect of splitter shape on interference effects (pressure recovery)

Printed in England for Her Majesty's Office by the Royal Aircraft Establishment, Farnborough. Dd.501371. K.4.

DETACHABLE ABSTRACT CARD

A.R.C. C.P. No. 1122
December 1968

Dobson, M. D.

533.693.3 :
621.43.033.2 :
533.693.49 :
532.526

TESTS AT A MACH NUMBER OF 2.0 ON A RECTANGULAR, TWIN-DUCT AIR INTAKE WITH VARIABLE GEOMETRY, SITUATED IN THE FLOW FIELD OF A SLENDER WING

The tests were made in the 3ft x 3ft tunnel to assess the performance of a rectangular twin-duct intake, including effects of limited immersion of the intake into a wing boundary layer. The effects in one duct, arising from interference caused by varying the flow through the other, have also been investigated.

Partial immersion of the intake into the wing boundary layer causes little degradation of the intake performance and indeed, small increases of pressure recovery are noted.

(Over)

A.R.C. C.P. No. 1122
December 1968

Dobson, M. D.

533.693.3 :
621.43.033.2 :
533.693.49 :
532.526

TESTS AT A MACH NUMBER OF 2.0 ON A RECTANGULAR, TWIN-DUCT AIR INTAKE WITH VARIABLE GEOMETRY, SITUATED IN THE FLOW FIELD OF A SLENDER WING

The tests were made in the 3ft x 3ft tunnel to assess the performance of a rectangular twin-duct intake, including effects of limited immersion of the intake into a wing boundary layer. The effects in one duct, arising from interference caused by varying the flow through the other, have also been investigated.

Partial immersion of the intake into the wing boundary layer causes little degradation of the intake performance and indeed, small increases of pressure recovery are noted.

(Over)

It is inferred from the results that interference effects may be sensitive to small crossflow angles at the intake. Smaller margins of mass flow reduction without interference are observed when the windward duct is throttled. The design of the leading edge of the wall which separates the two ducts (splitter), affects the interference characteristics and the present design is shown to be a considerable improvement over shapes tested previously.

It is inferred from the results that interference effects may be sensitive to small crossflow angles at the intake. Smaller margins of mass flow reduction without interference are observed when the windward duct is throttled. The design of the leading edge of the wall which separates the two ducts (splitter), affects the interference characteristics and the present design is shown to be a considerable improvement over shapes tested previously.

Published by
HER MAJESTY'S STATIONERY OFFICE

To be purchased from
49 High Holborn, London W C 1
13a Castle Street, Edinburgh EH 2 3AR
109 St Mary Street, Cardiff CF1 1JW
Brazennose Street, Manchester 2
50 Fairfax Street, Bristol BS1 3DE
258 Broad Street, Birmingham 1
7 Linenhall Street, Belfast BT2 8AY
or through any bookseller

C.P. No. 1122

SBN 11 470310 8